Available online at www.sciencedirect.com
ScienceDirect
Progress in Surface Science 82 (2007) 244–292
Progress in SURFACE SCIENCE
www.elsevier.com/locate/progsurf

Review

Excited states in the alkali/noble metal surface systems: A model system for the study of charge transfer dynamics at surfaces

J.P. Gauyacq [a,*], A.G. Borisov [a], M. Bauer [b,1]

[a] *Laboratoire des Collisions Atomiques et Moléculaires, Unité Mixte de Recherche CNRS-Université Paris Sud UMR 8625, Bât 351, Université Paris-Sud, 91405 Orsay Cedex, France*
[b] *Fachbereich Physik, TU Kaiserslautern, 67663 Kaiserslautern, Germany*

Abstract

The low coverage adsorption of alkalis on metal surfaces induces excited states localised on the adsorbate. In the case of noble metal substrates, these excited states can exhibit a very long lifetime, up to tens of fs in the Cs/Cu(1 1 1) system. We review recent experimental and theoretical investigations of alkalis adsorbed on noble metal surfaces, with emphasis on the characteristics of the alkali-induced excited states, the origin of their long lifetimes, and the consequences for the adsorbate dynamics. The possibility of long-lived resonances in other adsorbate/substrate systems is also discussed.

Contents

* Corresponding author. Tel.: +33 1 69157863; fax: +33 1 69156565.
E-mail address: jean-pierre.gauyacq@u-psud.fr (J.P. Gauyacq).
[1] Present address: Institut für Experimentelle und Angewandte Physik, Universität Kiel, 24098 Kiel, Germany.

0079-6816/$ - see front matter © 2007 Elsevier Ltd. All rights reserved.
doi:10.1016/j.progsurf.2007.03.006

1. Introduction

Quite a few electron- or photon-induced reactions in adsorbate–substrate systems involve an excited electronic state as a reaction intermediate [1–8]. A transient excited electronic state can be formed on an adsorbate directly by the incident particle, via electronic excitation, electron attachment or photo-excitation. An adsorbate excited state can also be formed through an indirect scheme, in which the energy of the incident electron or photon is absorbed by the substrate to form hot electrons, which in turn lead to the excitation of the adsorbate. All these reaction processes can involve single or multiple events (see the DIET/DIMET discussion in Ref. [9]). The excited state mediated reactions have been the subject of growing interest in the past years. In particular, the use of femtosecond

lasers to trigger and/or analyse the reaction directly in the time domain opened up a lot of fascinating possibilities in the field of surface chemistry studies.

In a reaction mediated by a transient excited electronic state (a resonant state), the formation of the excited state triggers an evolution in the adsorbate–substrate system, i.e., an energy transfer between the excited electrons and the nuclei. This process possibly leads to a rearrangement of the nuclei, opening the way to a variety of phenomena: vibrational excitation, dissociation, desorption or more generally, chemical reactions. In this context, the characteristics of the transient electronic state are of paramount importance. The energy of the excited state governs its accessibility for a given initial excitation and determines which final states can be reached. Most importantly, the excited state lifetime governs the efficiency of the reaction process. Indeed, a too short lifetime severely hinders the efficiency of the energy transfer and quenches the chemical reaction pathway. On the other hand, very long-lived states can be seen as very efficient reaction intermediates.

Recently, very long-lived excited states [10–12] have been observed in the case of alkali adsorbates on noble metal surfaces. As discussed below, such long-lived states were unexpected in these systems. It is, therefore, important to measure, characterise and analyse all the relevant parameters that govern the excited state lifetime and energy on a surface, with particular emphasis on the occurrence of long-lived states. The understanding of the origin of long-lived states opens extremely interesting new possibilities towards the control of reactions at surfaces.

In this context, the alkali/noble metal system presents a few very attractive features for such a study:

(1) The resonant states exhibit a relatively long lifetime, which is accessible by real-time measurements such as time-resolved two-photon photoemission spectroscopy (TR-2PPE).
(2) The system is experimentally well defined and tuneable with respect to a variety of parameters (surface, alkali species, and alkali coverage).
(3) The system can be modelled in a parameter-free approach. It is possible to study both the static situation (fixed adsorbate–surface distance) and, most importantly for a long-lived state, the dynamic situation where the excited adsorbate moves with respect to the surface.
(4) Some studies of the neutralisation of alkali positive ions by collision on noble metal surfaces have also been performed recently. This process is very closely related to the decay of excited states in the alkali/noble metal systems and thus probes the same phenomena from a different point of view.

Before going into the analysis of the excited state dynamics in the alkali/noble metal systems, one may recall the three types of processes that can be responsible for the decay of excited states at metal surfaces.

The first process is the one-electron transfer process, called resonant charge transfer (RCT), in which an excited electron localised on an adsorbate is transferred into the metal. It can be viewed as the tunnelling of the active electron through the potential barrier separating the atomic potential well from the metal potential well. This one-electron process is energy conserving and corresponds to the decay of an adsorbate state into unoccupied metal states of the same energy. When it is energetically possible, the RCT is usually very efficient since it involves one-electron coupling terms. Typically, at adsorption distances,

decay rates reach the eV range for a free-electron metal substrate, corresponding to sub-fs lifetimes. Compared to these values for a jellium metal, the long lifetimes, up to a few tens of fs, observed in the alkali/noble metals systems [10–12] appeared quite surprising. As we will see below, the long lifetime in the alkali/noble metal systems can be understood as an effect of the projected band gap of the noble metal surfaces which partially blocks the RCT [13]. RCT has been the subject of many studies in various contexts, in particular collisional charge transfer [14]. In the case of a metal described in the free-electron approximation, quantitative methods to treat the RCT process are now available [15–19] that can accurately account for the experimental observations [20–22]. Below, we will present results obtained with an extension of one of these methods (wave-packet propagation [17]) to the case of noble metal surfaces.

A second decay process involves the inelastic interaction between the active electron and the substrate electrons. In contrast to RCT, this process does not conserve the energy of a given electron, but corresponds to an energy decay process. It is associated with multi-electron coupling terms and, as such, can be considered weaker than a typical one-electron RCT process. Nevertheless, it plays a very important role in a variety of problems: decay of hot electrons in metals [23], decay of image states at surfaces [24,25], Auger neutralisation of positive ions at surfaces [26–29], or plasmon-assisted neutralisation of positive ions at surfaces [28,30–32]. As we will see below, multi-electron interactions significantly contribute to the decay of excited states localised on adsorbates when the RCT process is hindered.

As a last decay process for excited electrons at surfaces, one can mention the energy transfer from the electron to the heavy particle motion, such as the phonon excitation which plays a role in the decay of low energy excited electrons in metals [33,34], overlayer quantum wells [35,36] or in the decay of holes (electrons) in surface (image) states [37–40]. This process is usually considered to be weaker than the others and plays a role when those are inefficient. At this point, one can stress that the excited state mediated reaction mechanisms mentioned above involve an energy transfer from an electron to the heavy particles and can also be considered as a decay process of the excited state that can be included in this last category.

The scope of this review is to summarise the present state of our understanding of long-lived excited adsorbate resonances from an experimental and theoretical point of view. The outline of the review is the following. After a general presentation of the main features of the alkali/metal systems in Section 2, Section 3 is devoted to the experimental and theoretical methods applied to study the alkali/metal systems, with a strong emphasis on the noble metal substrates. Section 4 then presents the main experimental and theoretical results of the time evolution of the excited states in the alkali/noble metal systems; a lot of attention is given to the origin of a long-lived excited state in certain systems. Section 5 extends the discussion to other adsorbate systems where long-lived states have been (have not been) observed or predicted and to the perspective of control of these excited states.

2. General presentation of the alkali/noble metal adsorption system

2.1. General considerations

Alkali adsorption on metals has attracted much theoretical and experimental attention over several decades (for an overview on different aspects of alkali adsorption see reference

[41,42]). The most striking effect of alkali adsorption on metals is the drastic change of the surface work function. Typically, at low coverage, the work function drops quickly when the coverage increases, reaches a minimum around half the monolayer coverage and then increases, while remaining a few eV below the clean surface value. The first interpretation of this effect was given by Gurney [43], who explained that, since the alkali ionisation energy is smaller than the clean surface work function, the first alkalis adsorb as positive ions on the metal, thus leading to a dipole layer on the surface. This view was confirmed by early theoretical studies of adsorption of a single alkali atom on a jellium metal, showing a charge transfer from the adsorbate to the substrate [44]. As the coverage increases, the adsorbates progressively neutralise leading to saturation of the work function change, and for even higher coverage to a metallic layer [43]. This interpretation has been and is still much used to describe alkali adsorption. It was challenged a few years ago following theoretical studies on finite adsorption coverage on metals [45,46] and photoemission experiments [47], the idea being that an adsorbed alkali looks more like a strongly polarised alkali atom than like a positive ion. Further theoretical studies and analysis in the case of a single alkali on a metal surface [48–50] confirmed that Gurney's picture is appropriate. Qualitatively, one can say that a positively charged adsorbate induces an image charge in the metal. These screening charges are located at the surface and, for small adsorbate–surface distances, the whole system (ion + screening charge) can look like a polarised alkali atom [48,49], therefore the discussion on ionised or polarised adsorbates is partly semantic. Nevertheless, it has some importance in the present case. Indeed, at very low coverage, in Gurney's picture, an excited state can be formed by bringing an electron on the lowest unoccupied atomic orbitals of the alkali, even though it is much distorted by the metal neighbourhood, we will see below that the experimental observations of long-lived excited states can be interpreted in this way. At higher coverage, various phenomena can appear, depolarisation of the layer [43], island formation [51,52], alloying [53] or interstitial adsorption [54], making the situation more complex to describe. In the case of a complete mono-layer on the surface, the adsorbate alkali layer has a metallic character and quantum well states corresponding to quantisation of the electron motion in the layer can appear [55–57]. Theoretical descriptions of the overlayer quantum well structures have been reported, based on both model representations of the alkali overlayer [36,55,58,59] and on first principle calculations [60]. These studies account for the observed behaviours of these states. It must be stressed that the physical properties of a metallic overlayer of alkali on a metal are quite different from those of dispersed alkali atoms adsorbed on a metal, which forms the subject of the present review.

2.2. Excited state spectrum of alkali adsorption

The excited state spectrum of alkali covered surfaces has been investigated by a number of experimental groups. The typical techniques used for such studies are inverse photoemission spectroscopy (IPES), two-photon photoemission spectroscopy (2PPE), electron energy loss spectroscopy (EELS) and second harmonic generation (SHG) [61–65]. These complementary techniques revealed that the entire electronic surface structure becomes modified as a result of alkali adsorption even for coverages[2] of a fraction of a monolayer.

[2] In the following, all coverage values will be given with respect to the adsorbate saturation coverage, i.e., a closely packed alkali layer (1 ML) on the substrate.

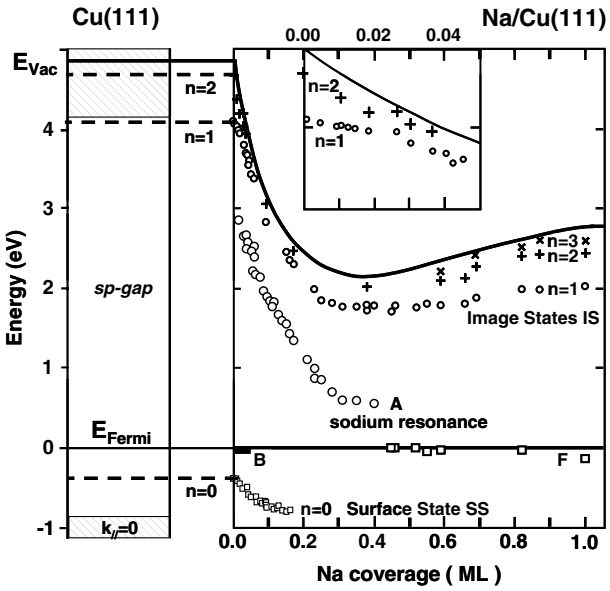

Fig. 1. Band scheme of the clean copper surface at $k_{\|} = 0$ (left) in comparison to the excited electronic states of the Na/Cu(1 1 1) system as function of Na coverage obtained from 2PPE experiments (right; reprinted from reference [66], Copyright (1994), with permission from Elsevier). The Cu(1 1 1) surface is characterized by the surface projected sp-band gap and the $n = 0$ Shockley surface state (SS) at a binding energy of 390 meV at 300 K with respect to the Fermi-energy E_F. The dashed lines close to the vacuum energy E_{Vac} indicate the energies of the ($n = 1$) and ($n = 2$) image states. Alkali adsorption results in a drastic change of the surface vacuum energy E_{Vac} (solid line) and of the binding energies of the image states ($n = 1$, $n = 2$, $n = 3$) as well as the Shockley surface state. Furthermore, a new adsorbate related state (A) appears in the spectrum.

Fig. 1 from Ref. [66] is the result of a 2PPE experiment on the Na/Cu(1 1 1) system. It illustrates different features of the excited electronic structure of the alkali/metal surface systems at low coverage.

1. The most apparent effect is the drastic change in the work function $\Phi(\theta)$ of the surface as a function of the alkali coverage, θ (upper solid line in Fig. 1). It arises from the strong dipole moment induced by the positive alkali core and its image charge at the surface. For low coverages the work function change is proportional to the number of dipoles at the surface and, therefore, proportional to coverage. At higher coverage alkali–alkali interaction becomes important as it reduces the effective dipole moment per alkali. An increasing deviation from the linear $\Phi(\theta)$ can be observed. At about half a monolayer this depolarisation effect has compensated the net dipole moment per alkali atom. With increasing coverage the work function increases until about 1ML coverage where a work function close to the value for the bulk alkali is observed.
2. Substrate-derived image-potential states ($n = 1$, $n = 2$, and $n = 3$), which already exist at the uncovered metal surfaces, are also strongly influenced by alkali adsorption. These states are excited states of electrons in front of metal surfaces that are bound in the attractive image potential well, when a surface projected band gap prevents the electron penetration inside the bulk [24,25]. As shown in Fig. 1, significant variations in the

binding energy of image-states are observed, in particular in the low coverage range represented in the inset. A comprehensive review of the behaviour of image-potential states on clean surfaces and after adsorption of alkali atoms can be found in reference [67].

3. The $n = 0$ state in Fig. 1 corresponds to the Shockley surface state SS of Cu(1 1 1). Surface states appear in gaps of the bulk electronic structure. They are localised close to the surface and present a parabolic dispersion with a mass usually different from that of the free electron [68]. The energy of this state decreases with increasing alkali coverage and the state finally disappears from the photoemission spectra as soon as it crosses the low energy edge of the $L_{2'} - L_1$ Cu(1 1 1) band gap located at about 0.9 eV below E_F at the $L_{2'}$ point.
4. Three alkali-induced states can be identified in Fig. 1. In the very low coverage regime an occupied state B is observed, it is completely absent above 0.1 ML coverage. At coverages below half a monolayer, an unoccupied state A is very clearly visible in the 2PPE spectra. Its energy rapidly decreases with the change of the surface work function. Close to the work function minimum, the state A suddenly disappears and a new occupied state F shows up right at the Fermi edge and remains for coverages beyond 1 ML.

The latter three states (A, B and F) do not exist at the clean Cu surface. Therefore, these features can be directly related to the adsorbed alkali atoms. The appearance of the low coverage state A and its shift to lower excitation energies when the coverage increases have been observed for a number of alkali adsorption systems. Sudden changes in the electronic structure at finite coverage, as observed in Fig. 1 at about half a mono-layer, have been reported in several articles and are typically connected with the appearance of an ordered alkali over-layer structure observable by LEED [58,69–71]. The details in the related electronic structure in this coverage regime seem to vary from system to system and may critically depend on the balance between alkali–substrate and alkali–alkali interaction which becomes relevant as an ordered over-layer develops. For the example given in Fig. 1, the observation of an energy level right at the Fermi edge probably indicates the presence of the metallic phase of the alkali over-layer which is expected to appear when the first monolayer approaches completion.

For the rest of the paper we will mainly focus on the feature A which appears in the case of Na/Cu(1 1 1) at about 3 eV above the Fermi level in the zero coverage limit.

The dependence of the properties of the excited state A on a variety of parameters such as substrate material, substrate orientation, alkali species, momentum and coverage dependence has been investigated in the past. These results revealed a general behaviour of this state that is qualitatively more or less independent of the substrate species, substrate orientation and alkali species:

(1) The excited state A has been identified in several alkali/surface systems investigated by IPE and 2PPE [11,72–74,63,75,76]. In addition, EELS and SHG experiments give indirect indications for the existence of this state [61,65]. In the zero coverage limit, this state is typically located several eV above E_F.
(2) The energy of the excited state shows a strong coverage dependence, its excitation energy with respect to the Fermi level decreases monotonically with coverage (see e.g., Ref. [64,66,72,76] and Fig. 1). As will be discussed later, this energy shift is a direct consequence of the interaction with the field of the neighbouring alkalis.

(3) As a result of the weak interaction between separated alkali adsorbates, at low coverage no $k_{\|}$-dispersion of the alkali excitation is expected. This has been verified experimentally for Cs/Cu(1 1 1) [72], Cs/Cu(1 0 0) [72] and Cs/Ag(1 1 1) [77]. For higher coverage, wave-function overlap between neighbouring alkalis should give rise to dispersion. At 0.33 ML, a $k_{\|}$-dispersion has been observed for K/Ag(1 1 0) [63]. However, the measured effective mass of 2.3 m_e shows that the wave function overlap between neighbouring adsorbates is still weak at this coverage.
(4) The symmetry properties of the state have been studied for Cs/Cu(1 1 1) by means of polarisation dependent 2PPE [78]. It could be shown that the corresponding excited state is invariant under rotation around the surface normal.
(5) The spectral width of the state measured at room temperature lies typically in the range of several 100 meV [11,66,75,79]. For Cs/Cu(1 1 1) at 33 K a much narrower line width of 70 meV has been reported [12]. Line shape measurements at room temperature indicate a dominant contribution due to inhomogeneous broadening. The origin of inhomogeneous broadening of alkali line shapes has been discussed earlier by Wertheim et al. [80] and Petek et al. [79] and was attributed to the excitation of frustrated translation modes and to the high mobility of the alkalis at the surface at elevated temperatures. Measurements at 33 K allowed a deconvolution of the actual homogeneous contribution to the line shape [79], related to the total dephasing of the alkali excitation.

Four different alkali/metal surface systems that highlight some common properties and differences of alkali adsorption in the low coverage regime are compared in Table 1. The respective parameters changed are alkali species (Cs/Cu(1 1 1) vs. Na/Cu(1 1 1)), substrate orientation (Cs/Cu(1 1 1) vs. Cs/Cu(1 0 0)) and substrate species (Cs/Cu(1 1 1) and Cs/Ag(1 1 1)). Note that for all four substrates, there exists a surface projected band gap and the excited state lies within it. Table 1 illustrates the rather general properties of the excited states in the alkali/metal systems that were outlined above. As an additional feature, one can notice that the energy position of the alkali resonance with respect to the Fermi level is almost the same in the four systems. The coverage dependence of the alkali resonance energy is rather steep and varies from one system to another. This variation is not exactly linear with the coverage (see illustration and discussions below in Section 4.1.3) and the value quoted in the fourth column is an average slope.

Table 1
Some static properties of the investigated alkali resonance for different adsorption systems: E_0 is the resonance energy with respect to E_F for vanishingly small adsorbate coverage, FWHM is the measured spectral width of the resonance (the values at 33 K and the value for Cs/Ag(1 1 1) in brackets correspond to the deconvoluted pure homogeneous broadening), $dE/d\theta$ is the change in resonance energy with alkali coverage at low coverages

System	E_0 [eV]	FWHM [meV]	$dE/d\theta$ [eV/ML]
Na/Cu(1 1 1) [66]	3.0	410 ± 30, RT	9
Cs/Cu(1 1 1)	3.1	350 ± 50, RT [11] 70 ± 10, 33 K [12]	8.5
Cs/Cu(1 0 0)	3.15	400 ± 50, RT [11] 250 ± 20, 33 K [79]	4.5
Cs/Ag(1 1 1)	2.7	<420 [11] (90 meV [77])	

Despite the existence of rather general properties for the excited states in all the alkali/metal systems that were studied, the assignment of the resonance localised on the alkali (peak A in Fig. 1) to a specific orbital of the free alkali atom was not obvious and different answers were given in different works. Most of the assignments were based on the energy position of the alkali resonance in the limit of very low coverage. In several publications, the observed excitation was attributed to the lowest excited p_z orbital of the free atom or to an hybrid orbital with a large component on this p_z orbital [66,72,73,63] (p_z refers to the p orbital aligned along the surface normal, the other two p sublevels are noted p_x and p_y). This assignment was based on a comparison of the resonance energy to that found in early theoretical studies on alkali/metal systems: Li/Jellium [44], Na/Jellium [81,82] and K/Jellium [81]. These considered the case of a single alkali atom adsorbed above a free-electron metal surface, either via a density functional approach [44] or a model study [82]. In these calculations, the lowest excited resonance was found to be very broad (width of the order of 1 eV) and was assigned to the outer s orbital of the free alkali atom, however strongly mixed with the next p_z orbital. The hybridisation was caused by the interaction with the metal and the resonance energy was found to shift rather rapidly in energy, as the adsorption height was varied [82,83,15,84,21]. The calculated energy position of this lowest lying resonance, typically around 1 eV above the Fermi level, was too low to account for the experimental observations. Therefore, it was tempting to assign the observed resonance to a higher lying state, either the p_z orbital (or a hybrid with a large p_z component), or the $p_{x,y}$ orbital. The problem was then the lack in most experiments of a lower lying state that could be assigned to the lowest s,p hybrid. Because of this absence, Nielsen and Thowladda [75] made an opposite choice and assigned the resonance observed in K/Al(1 1 1) to the 4s orbital of the alkali, despite its rather large energy, 2.4 eV, above the Fermi level. In only one IPES experiment [76] on Li, Na and K/Al(1 1 1), a second lower lying resonance (although much weaker) could be observed around 0.7 eV above the Fermi level; the observed energies in the limit of very low coverage were close to the theoretical results [81,82] and the two peaks were then attributed to the s and p levels of the free alkali atom. Finally, one must also mention the case of the Cs/Cu(1 1 1) system where the lowest s, p_z hybrid was found by Muscat and Newns [82] to be significantly higher in energy than for the lighter alkalis, so that it was consistent with the experimental observations [10] and the observed resonance could be assigned in that case to the lowest s, p_z hybrid. Similarly, for the Cs/Al(1 1 1) system, the same assignment is supported by recent calculations [85] which found the lowest excited state at 2.3 eV above the Fermi level with a width around 1 eV, in quite satisfying agreement with the experimental observations of Frank et al. [76] in the limit of low coverage. A rather different assignment method was used by Arena et al. [74]. From the analysis of the electron energy dependence of the signal intensity in an IPES experiment, they concluded that the Cs resonance at Cu(1 0 0) and Cu(1 1 1) surfaces was compatible with a d_z orbital of cesium.

Below, we concentrate mainly on the excited state localised on the alkali in the case of noble metal surfaces. We show that model theoretical studies account for the experimental observations (energies and lifetimes of the alkali resonances). This allows assigning unambiguously the observed resonance to the lowest excited state on the alkali. It corresponds to a hybrid of the different orbitals of the free atom (mainly s and p) which correlates to the alkali ground state (s symmetry) when the alkali–substrate distance goes to infinity. Experimentally, up to now, no higher lying state has been observed in these systems and this point is addressed below. From the success of the studies on noble metals, we

could conclude that the same assignment should also hold for the other substrates. However, this tentative assignment has to be supported by further theoretical studies. Recent test calculations (unpublished) on the case of Na and K adsorbed above a free-electron Al surface, using the approach outlined below for the noble metal substrates, yielded an energy for the lowest lying alkali-localised resonance around 2.7 eV above the Fermi level in both systems, with a width larger than 1 eV. This value is consistent with the experimental energy position of the alkali-induced resonance in the limit of very low coverage [76]. This allows assigning the main experimentally observed alkali resonance to the lowest excited state on the adsorbed alkali, both for noble metals and free-electron substrates. The difference between these results and earlier theoretical studies on Al are attributed, besides the fact that they use different approaches, to the consideration of different adsorption distances [81,82] and to the effect of different treatments of the image charge interactions. However, the problem of the assignment of the very weak structure observed on Al(1 1 1) substrates at an energy lower than the lowest alkali resonance is still remaining. [76]. Further theoretical and experimental analysis is required to fully solve this problem. In this context, one can mention possible complications coming from the specificity of the alkali adsorption in some systems such as Al(1 1 1), where interstitial adsorption and island growth have been reported to occur above a certain alkali coverage [52,86,51,87], possibly leading to the co-existence of different adsorption states of the alkali.

3. Methods

3.1. Experimental

3.1.1. Time-resolved two-photon photoemission spectroscopy

To measure the lifetime (in particular the depopulation time) of excited adsorbate resonances within a real-time experiment, high resolution pump–probe experiments capable of a time resolution in the low femtosecond regime are required. So far, the decay dynamics of the alkali resonance introduced in the last section has been investigated by means of time-resolved two-photon photoemission (TR-2PPE) and interferometric and time-resolved two-photon photoemission (I2PC). A comprehensive review of different aspects of these two techniques is given in reference [88]. In the following a short summary of these techniques will be given.

3.1.1.1. Experimental setup. The principle of time-resolved two-photon photoemission spectroscopy is based on an optical pump–probe scheme that allows for a time resolution that is mainly determined by the pulse width and stability of the exciting pulsed laser source. An overview of a typical experimental setup used for investigations presented in this paper is given in Fig. 2. A femtosecond laser pulse incident onto a surface populates an unoccupied electronic level located between Fermi edge and vacuum level. A second laser pulse probes the population of this excited state by photoemission into the vacuum, where the electrons can be detected by an energy discriminating electron analyzer. This 2PPE configuration allows for spectroscopy of excited (usually unoccupied) electron states at high energy resolution of the order of 50 meV. This static 2PPE mode already allows line width measurements and enables in principle the determination of the total dephasing time T_2 of the excitation process, if inhomogeneous broadening can be neglected or accounted for. In a time-resolved mode, an optical delay stage is implemented into the

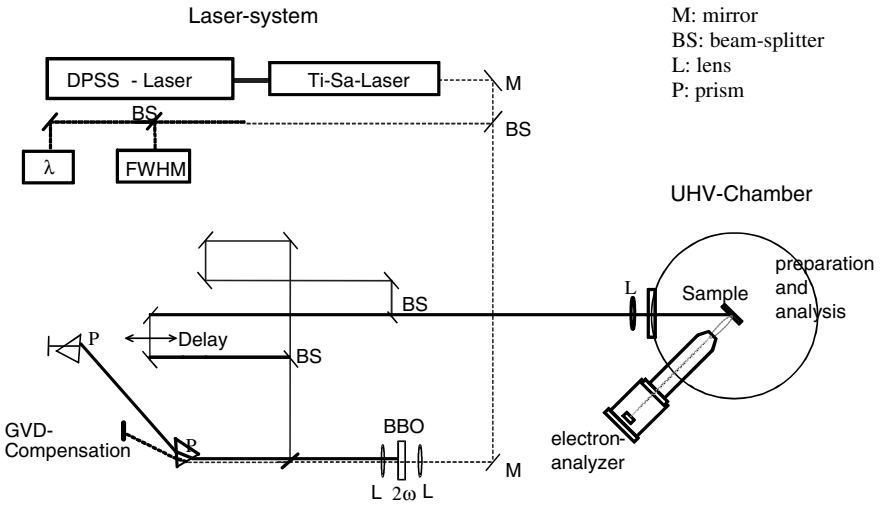

Fig. 2. Schematic view of an experimental set-up for time-resolved two-photon photoemission. The dashed line marks the path of the red output of the Ti-Sapphire laser; the solid line corresponds to the frequency-doubled light initiating the photoemission process at the sample surface. The optical delay line in one of the two beam paths of the second harmonic is used to adjust the temporal delay between pump and probe line on a femtosecond time scale.

setup that enables the defined control of the temporal delay between pump and probe pulses. This additional degree of freedom allows to successively probe the remaining population of the excited state at different times after excitation by the first laser pulse. The resulting photoemission signal recorded as function of the temporal delay between pump and probe laser pulse at a fixed kinetic electron energy is referred to as the correlation trace of the time-resolved experiment. In case of equal pump and probe pulse – as typically used for the investigation of the lifetime of alkali resonances – this trace is referred to as the autocorrelation trace of the measurement (see e.g. Fig. 4). When the temporal delay can be adjusted with a sub-femtosecond accuracy (corresponding to reproducible control of the delay stage in the 10 nanometer regime) interferometric time-resolved 2PPE can be performed. Oscillations (fringes) in the 2PPE yield as a function of temporal delay reflect constructive and destructive interferences of the pump and probe pulses around time-zero. This degree of accuracy can further increase the information depth in particular with respect to the dephasing of laser field and involved electronic states and, therefore, it allows a real-time access to the total dephasing time T_2.

3.1.1.2. Data evaluation. In general, the experimental signal from a TR-2PPE scan is a convolution of the autocorrelation trace of the exciting laser pulses and of the decay dynamics of the probed electronic excitation. In the absence of coherence in the excitation process, TR-2PPE probes the pure population decay of the excited state and the experimental trace can be modeled within a simple rate equation approach. If coherence between the electromagnetic field and the electronic transitions involved in the 2PPE process persists for a finite time (finite with respect to the laser pulse width), decay of electron population and decay of the polarization induced by the laser field are probed in the experiment

and contribute to the detailed shape of the 2PPE signal. A more realistic approach to model the measured traces for this case can be performed within the framework of density matrix formalism. In order to simulate the dynamical processes involved in TR-2PPE, Hertel et al. [89] applied this formalism to a two-level system, representing the initial and intermediate states of the 2PPE process. This model can be expanded to three discrete levels, corresponding to *discrete* initial, intermediate and final states of the 2PPE process, interacting with an electromagnetic field.

To deconvolute the relevant dynamical parameters of interest (lifetime and dephasing of the intermediate state involved in the 2PPE process, i.e. the alkali excitation) the experimental data are fitted by the Liouville–von Neumann equation that describes the temporal evolution of the density matrix of the system:

$$\frac{\mathrm{d}}{\mathrm{d}t}\hat{\rho} = -\frac{\mathrm{i}}{\hbar}[\widehat{H}, \hat{\rho}] + \frac{\mathrm{d}}{\mathrm{d}t}\hat{\rho}^{\mathrm{diss}}. \tag{1}$$

Here the density matrix $\hat{\rho}$ is defined by its elements $(\hat{\rho})_{nm} = |n\rangle\langle m|$ and $[\widehat{H}, \hat{\rho}]$ is the commutator of the $\hat{\mathrm{H}}$ and $\hat{\rho}$ operators. The diagonal elements $(\hat{\rho})_{nn}$ give the probability of the system being in the state $|n\rangle$, while $(\hat{\rho})_{nm} = (\hat{\rho})^*_{mn}$ represent the optically induced coherence between $|n\rangle$ and $|m\rangle$ states. The dissipative term $\frac{\mathrm{d}}{\mathrm{d}t}\hat{\rho}^{\mathrm{diss}}$ describes the temporal decay of the respective elements of the density matrix due to coupling to an external bath. For a known laser field envelope, the remaining parameters for a fitting procedure are the depopulation time T_1 and the dephasing time T_2 of the electronic states involved in the 2PPE process. Dephasing corresponds to the decay of the coherence between the various states in the system. It can occur both with and without population decay and one can define a pure-dephasing time T_2^* associated to coherence decay without population decay. The various dephasing times are linked by: $1/T_2 = 1/T_2^* + 1/2T_1$. Certain assumptions may be made to reduce the set of free parameters. For example, for the case of excitation from/into a band it can be shown that the corresponding step can be treated in the limit of rapid dephasing ($T_2 \to 0$ fs) [90]. In the comparisons with theoretical results below, we only consider the depopulation time T_1 of the alkali excitation (intermediate state). However, the knowledge of T_2 is required for an accurate determination of T_1. If a value of T_2 is unavailable, considering the two limiting cases, vanishing T_2 or T_2 equal to twice T_1, can yield an error bar for the T_1 experimental value.

We will see later that the 2PPE signal from the adsorbate is not only governed by the pure electron dynamics but to a certain extent also by the adsorbate motion induced by the electronic excitation. A detailed quantitative comparison between theory and experiment requires, therefore, the explicit consideration of the nucleus dynamics. This issue will be discussed in more detail in Section 4.2.3.

3.1.2. First time-resolved results

The very general behaviour of the alkali excitation at a surface and the variety of parameters available for tuning of this system offer an ideal tool for systematic studies of charge transfer mediated surface processes involving an adsorbate resonance. In addition to the static properties presented above, it was found that for certain systems the alkali resonance exhibits a surprisingly long lifetime accessible by time-resolved 2PPE. This specific behaviour was observed for the first time for excited Cs adsorbed on Cu(1 1 1) [10]. The top graph of Fig. 3 shows a color coded 2PPE map of Cs/Cu(1 1 1) recorded with an electron energy analyzer capable of parallel detection of energy and pho-

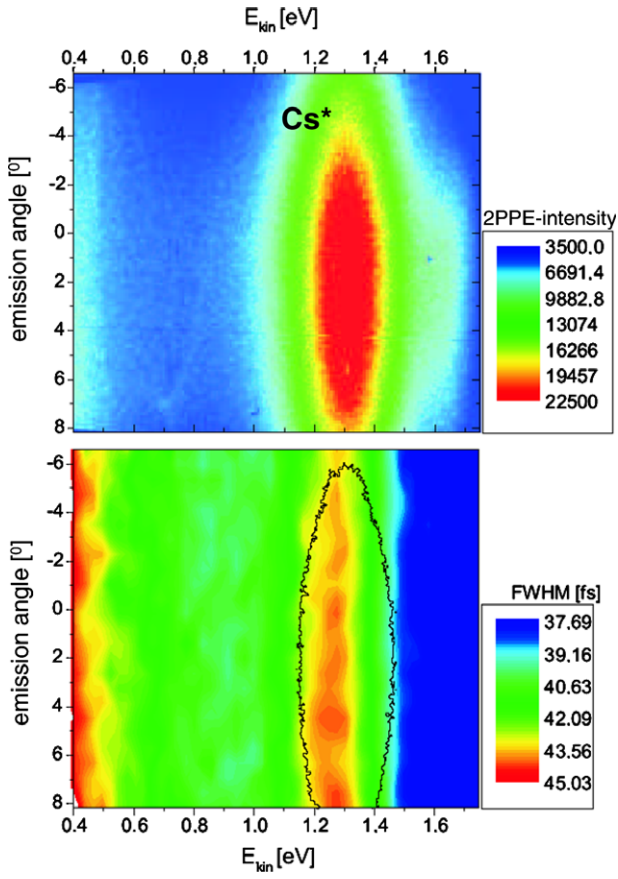

Fig. 3. Two-photon photoemission map and time resolved 2PPE map of Cs/Cu(1 1 1) recorded with an electron energy analyzer capable of parallel detection of energy and emission angle ϑ (with respect to the surface normal). The top graph shows a colour-coded 2PPE spectrum exhibiting the Cs-resonance at a measured electron kinetic energy of 1.3 eV. Due to the localisation of the Cs-state no dispersion of the resonance energy as function of the emission angle is observed. The bottom graph maps the FWHM of the 2PPE autocorrelation traces measured at each point in the E–ϑ plane. The FWHM of the autocorrelation trace can be considered as an indirect measure of the excited state lifetime. Clearly visible is the increase of the lifetime close to the position of the Cs-resonance (indicated by the black line in the bottom graph). The obvious downward shift in the lifetime maximum to lower energies in comparison to the resonance energy is a consequence of the adsorbate motion induced by the electronic excitation which will be discussed in Section 4.2 (from reference [205]).

toemission angle. Clearly visible is the alkali excitation at an electron kinetic energy of 1.3 eV. The Cs coverage for these measurements was 0.08 ML. The bottom graph shows the corresponding TR-2PPE data represented here by the FWHM of the 2PPE autocorrelation trace measured for each point of the top graph. The FWHM of the 2PPE autocorrelation trace can be considered as an indirect measure of the excited state lifetime. The FWHM maximum just below 1.3 eV kinetic energy highlights the enhanced lifetime of the Cs-resonance state. It was the longest ever observed lifetime for an electronic excitation of a metal chemisorption system. The corresponding autocorrelation trace as compared to the laser autocorrelation and to fits based on the Liouville von Neumann

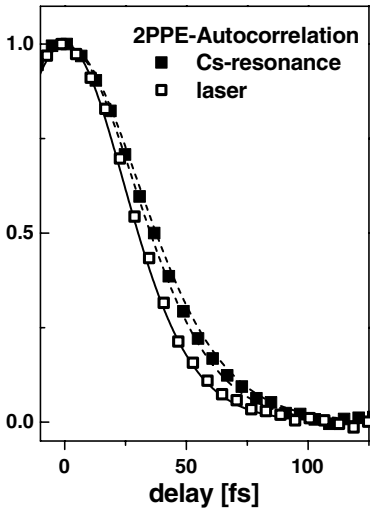

Fig. 4. Data analysis of a time-resolved 2PPE autocorrelation trace for the excited cesium state at a Cu(1 1 1) surface yielding a lifetime $T_1 = 12 \pm 3$ fs. The graph shows the measured autocorrelation trace for positive temporal delays (black squares) compared with traces calculated with $T_1 = 9$ fs and $T_1 = 14$ fs (dashed lines), assuming that the dephasing rate Γ_{23} is exclusively determined by T_1 ($\Gamma_{23} = (2T_1)^{-1}$). Open squares represent the laser autocorrelation measured by excitation from the Shockley surface state of the clean Cu(1 1 1) surface. The solid line is a fit to the laser autocorrelation with a pulse width of 39.5 fs.

formalism is shown in Fig. 4. The value of T_1 of 12 ± 3 fs (for $T_2 = 2 \times T_1$) deconvoluted from the measured autocorrelation trace contradicts markedly with theoretical results for free-electron metal substrates that predicted intrinsic line-widths of alkali resonances in the 1 eV range corresponding to sub-femto-second lifetimes for these excitations. It is this lifetime and its dependence on different system parameters, which are the focus of the following experimental and theoretical considerations.

3.2. Theoretical

For the case of a single adsorbate, a model approach of the alkali/metal systems that can treat the dynamics of the transient excited states observed in TR-2PPE has been developed. It was initially developed to treat the electron transfer process in the course of atom(ion)–metal surface collisions, where it was very successful, both for free-electron metal [20,21] and noble metal surfaces [91].

3.2.1. Description of the model

The method developed to treat the RCT has already been presented [92] and only a brief outline is given here. It consists of studying the resonant states of the adsorbate/metal substrate system via the model one-electron Hamiltonian:

$$H = T + V_{\mathrm{Surf}} + V_{\mathrm{Ads}} + \Delta V_{\mathrm{Surf}} \tag{2}$$

where T is the electron kinetic energy, V_{Surf} is the electron–clean metal surface interaction, V_{Ads} is the electron–adsorbate interaction and ΔV_{Surf} is the modification of the electron–metal interaction induced by the presence of the adsorbate. The Hamiltonian

(2) only includes a single adsorbate, so that it is representative of the low alkali coverage situation.

In the case of the alkali/metal systems, we assume that the alkali adsorbate is ionised on the surface and that the alkali core is not modified by the adsorption. We can therefore take V_{Ads} as the electron interaction with an alkali positive ion, as it can be obtained from earlier atomic physics studies. Similarly, in the Hamiltonian (2), we assume that the only modification of the V_{Surf} interaction, i.e., the ΔV_{Surf} term, corresponds to the electrical image of the alkali positive ion core. One can stress that the above Hamiltonian imposes the charge state of the alkali, thus allowing the computation of excited states. This is obviously well adapted for the computation of excited states corresponding to the capture of an electron by an ionised alkali.

In practice, for the results presented below, the V_{Ads} potential is taken as a pseudopotential of the Kleynman–Bylander form [93], built from the l-dependent pseudo-potentials by Bardsley [94]. More details can be found in Ref. [95]. For the electron–surface interaction potential, V_{Surf}, we used two different model potentials. The first one, well adapted to treat free-electron metal surfaces, uses the model potential derived by Jennings et al. [96]. This potential is only a function of z, the electron surface distance. It is an analytical expression that smoothly joins the image charge interaction in the vacuum with the bottom of the conduction band in the metal. The (1 1 1) and (1 0 0) surfaces of noble metals require a special treatment due to the peculiarities of their electronic structure: the presence of a projected band gap in the direction normal to the surface (L- and X-band gaps, see e.g., in [25]) and the existence of surface and image states. The projected band gap forbids electron propagation along the surface normal in a certain energy range and can thus influence the electron transfer between an adsorbate and the metal surface. To describe the (1 1 1) and (1 0 0) surfaces of the noble metals, we used the model description of V_{Surf} developed in Ref. [97,98] from ab initio studies. These potentials reproduce the surface electronic properties at the $\overline{\Gamma}$ point. They only depend on z, the electron coordinate normal to the surface and assume a free electron motion parallel to the surface.

3.2.2. Determination of the adsorbate localised excited states and of the decay due to resonant charge transfer (RCT)

Due to the presence of the continuum of metallic states, excited states localised on an alkali adsorbate appear as resonances, i.e., as quasi-stationary states that decay by electron transfer into the metal. A few non-perturbative quantum mechanical methods have been developed to solve the model Hamiltonian (2) in the case of a free-electron metal [15–19]. Most of the results presented here are obtained with a non-stationary approach: the wave-packet propagation (WPP) approach [17,92]. It consists of solving the time-dependent Schrödinger equation with Hamiltonian (2) to get the time dependent electron wave function $\Psi(\vec{r},t)$. Hamiltonian (2) is cylindrically symmetric around the axis normal to the surface that goes through the adsorbate and so, m, the projection of the electron momentum on the symmetry axis is a good quantum number. The electron wave function $\Psi(\vec{r},t)$ is represented on a mesh of points in cylindrical coordinates $\vec{r}=(\rho,\phi,z)$. The time propagation of the wave packet makes use of a split-operator approximation [99,100], which allows to treat separately and then in a well-adapted way the different terms in Hamiltonian (2) (see e.g., in [92]). A complex absorbing potential is introduced at the grid boundaries to suppress artificial reflections of the wave packet.

The time propagation starts with an initial electron wave function $\Psi(\vec{r}, t=0) = \Phi_0(\vec{r})$. From the time propagation, one can define the survival amplitude of the electron in the initial state:

$$A(t) = \langle \Phi_0(\vec{r}) | \Psi(\vec{r}, t) \rangle \tag{3}$$

from which one can get the density of states, projected on the initial state:

$$n(\omega) = Re\left(\lim_{\eta \to O^+} \frac{1}{\pi} \int_0^\infty \mathrm{e}^{\mathrm{i}\omega t} \mathrm{e}^{-\eta t} A(t)\, \mathrm{d}t \right) \tag{4}$$

All the excited states appear as peaks in the projected density of states. Within the WPP approach, the $e^{-\eta t}$ term is taken care of by the optical absorbing potential at the boundaries of the calculation grid, so that the projected density of states, $n(\omega)$, is given simply by $n(\omega) = Re\left(\frac{1}{\pi} \int_0^\infty \mathrm{e}^{\mathrm{i}\omega t} A(t)\, \mathrm{d}t\right)$. The size of a given peak is directly related to the weight of the resonance wave function in the initial wave function, $\Phi_0(\vec{r})$. In the present study, the excited states are strongly perturbed atomic states; nevertheless they still retain a significant overlap with the free Cs wave functions, so that the latter are a good choice for $\Phi_0(\vec{r})$. Direct analysis of $n(\omega)$ or of the time dependence of $A(t)$ yields the energy position, E_R, and the width of the resonances. In this case, the width is equal to the decay rate of the excited state via the RCT process and is noted Γ_{RCT}. The WPP calculation can also yield the resonance wave function, $\Phi_R(\vec{r})$, corresponding to the resonance located at E_R via:

$$\Phi_R(\vec{r}) = \lim_{\eta \to 0^+} \int_0^\infty \mathrm{e}^{\mathrm{i}E_R t} \mathrm{e}^{-\eta t} \Psi(\vec{r}, t)\, \mathrm{d}t \tag{5}$$

In practice, the wave packet propagation is performed up to a large but finite time, allowing convergence of the time integral in (4) and (5).

3.2.3. Electron–electron interaction

As stated in the introduction, besides the RCT, excited states also decay via inelastic electron–electron interactions. Below the corresponding decay rate is noted Γ_{ee}. Qualitatively, the excited electron makes a collision with one of the substrate electrons resulting in its scattering into metal states of lower energy.

Two methods have been used to evaluate Γ_{ee}. In the first one [101,102], the resonant wave function, $\Phi_R(\vec{r})$, determined in the previous section is used as the initial state in a perturbation calculation of Γ_{ee}:

$$\Gamma_{\mathrm{ee}} = -2 \int\int \mathrm{d}\vec{r}\mathrm{d}\vec{r}'\, \Phi_R^*(\vec{r}) \mathrm{Im}(\Sigma(\vec{r}, \vec{r}'; E_R)) \Phi_R(\vec{r}') \tag{6}$$

where Σ is the quasi-particle self-energy, evaluated in the GW approximation [23,103]. This many-body response theory approach is analogous to the one used for the study of image state decay on clean metal surfaces, which was very successful in accounting for experimental data (see details in [23,4]). In the GW approximation [103], one only considers the first term in the series expansion of the self energy, Σ, in terms of the screened Coulomb interaction, $W(\vec{r}, \vec{r}', E)$. The decay rate is then expressed as:

$$\Gamma_{\mathrm{ee}} = -2 \sum_{E_{n,\vec{k}}}^{E_0 \geqslant E_{n,\vec{k}} \geqslant E_F} \int\int \mathrm{d}\vec{r}\mathrm{d}\vec{r}'\, \Phi_R^*(\vec{r}) \psi_{n,\vec{k}}(\vec{r}) \mathrm{Im}(W(\vec{r}, \vec{r}'; E_0 - E_{n,\vec{k}}) \Phi_R(\vec{r}') \psi_{n,\vec{k}}^*(\vec{r}')$$

where $\psi^*_{n,\vec{k}}(\vec{r})$ are the wave functions of the final states participating in the decay (n is the band index and $\vec{k}$ is the electron momentum). The screened Coulomb interaction is obtained in the linear response theory as detailed in Ref. [23,104].

The second method is phenomenological and inspired by LEED treatments [105]. It consists of introducing into the WPP calculation a local complex potential inside the metal that mimics the effect of the inelastic electron–electron interaction. The decay rate that comes out of the WPP study then takes into account both the RCT and the multi-electron decay processes. The magnitude of this complex potential should a priori depend on the energy of the excited state. It can be obtained from the known lifetime of hot electrons in the bulk (e.g., [23,106,89]) or adjusted to results obtained from the above many-body theory.

The total decay rate of the excited state, Γ_T, is obtained as the sum of the two decay rates discussed above:

$$\Gamma_T = 1/\tau = \Gamma_{RCT} + \Gamma_{ee} \tag{7}$$

The lifetime of the excited state, τ, is given by the inverse of the total decay rate, Γ_T. The definition (7) makes the implicit assumption that the two decays are not influencing one another. This has been checked using the above phenomenological method: it appears that the total decay rate varies linearly with the effective complex potential, confirming the validity of the above summed expression and the independence of the two decay channels [101]. Further discussion of the expression (7) and its significance for a photoemission experiment will be given below. But, at this stage, one can stress that the two terms in (7) correspond to decays toward different kinds of final excited electronic states: Γ_{RCT} corresponds to an energy conserving transition of the excited electron whereas Γ_{ee} corresponds to a sharing of the excited electron energy with the substrate electrons, i.e., to a decay of the excited electron energy.

3.2.4. First results

As a first set of results, Fig. 5 presents the energy and RCT decay rate of Cs levels interacting with a metal surface as a function of Z, the Cs–surface distance, measured from the surface image reference plane [13,95]. Two different metal surfaces are considered: a free-electron metal with Cu characteristics and Cu(1 1 1). The results are presented for two different states of $m = 0$ symmetry, correlating at infinite separation to the 6s and 6p levels of Cs. Although the results presented in this section are specific to the Cs alkali, the other alkalis were found to behave qualitatively in the same way.

The energy of the levels is seen to be very similar on both surfaces, increasing when the alkali approaches the surface, roughly following the image charge interaction. The RCT decay rates, Γ_{RCT}, are quite different on the two surfaces. On a free electron metal, Γ_{RCT} for the various levels presented in Fig. 5 increases roughly exponentially as Z decreases from large Z and saturates at small Z. The Cs adsorption distance is 3.5 a_0, measured from the image plane, as it can be obtained from the coverage dependence of the work-function [61] or from LEED experiments [107]. At the adsorption distance on a free-electron metal, the RCT decay rate is of the order of 1 eV, corresponding to a lifetime of the excited state of the order of 0.5 fs. This value is typical of the RCT rates for an alkali on a free-electron metal, and agrees well with earlier self-consistent treatments of alkali adsorption on jellium surfaces [44,81,108]. One can also notice that the decay rate of the level correlating to the 6p Cs level at infinity is larger than that of the level correlating to the 6s level. This

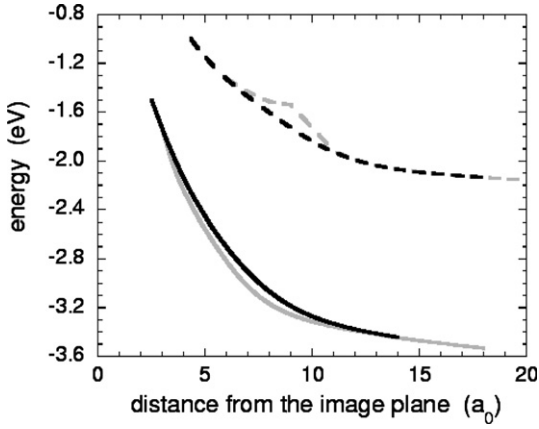

Fig. 5a. Energy of the lowest lying resonances of $m = 0$ symmetry in the Cs/Cu system as a function of the alkali–surface distance measured from the Cu image reference plane. The energy is given with respect to the vacuum level. Full lines: level correlated at infinite separation to the atomic Cs(6s) level. Dashed lines: level correlated at infinite separation to the atomic Cs(6p) level. Black lines: Cu(1 1 1) surface. Grey lines: free-electron metal surface.

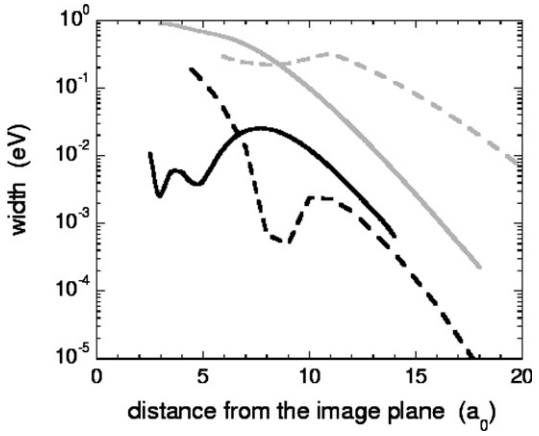

Fig. 5b. RCT decay rates (in eV) of the lowest lying levels of $m = 0$ symmetry in the Cs/Cu system as a function of the alkali–surface distance measured from the Cu image reference plane. Full lines: level correlated at infinite separation to the atomic Cs(6s) level. Dashed lines: level correlated at infinite separation to the atomic Cs(6p) level. Black lines: Cu(1 1 1) surface. Grey lines: free-electron metal surface.

difference is mainly attributed to the lower binding energy of the 6p level. It is thus associated with a more diffuse wave function allowing a larger overlap at large Z with the metal wave functions. One can also stress that the behaviour of the Cs level energy and RCT rate on a free-electron metal is very similar to what was found in other atom(ion)-free electron metal surface systems [15,16,20,21].

The situation on Cu(1 1 1) is quite different: the RCT decay rate, Γ_{RCT}, for the lowest state increases roughly exponentially as Z decreases from infinity and around 7 a_0, it drastically decreases down to very small values around 5–10 meV for Z distances in the adsorp-

tion distance range. The RCT rate for this state thus appears to be 2 orders of magnitude smaller on Cu(1 1 1) than that of its equivalent on a free-electron metal. In such a situation where the RCT rate is very low, one should wonder about the decay by inelastic electron–electron interaction. Γ_{ee} is usually much smaller than Γ_{RCT}, but if the latter is almost cancelled, then Γ_{ee} can play a significant role. Calculation of Γ_{ee} using a many-body response theory [101] for Cs/Cu(1 1 1) at the adsorption distance yields a value of 15 meV, i.e., a total lifetime of 30 fs. This calculation thus predicts the existence of a very long-lived state in Cs/Cu(1 1 1), much longer lived than on a free-electron metal. The long lifetime is due to the quasi-blocking of the RCT by the projected band gap of the Cu(1 1 1) surface (L-band gap) and the total decay rate of the excited state is dominated by the inelastic interaction with bulk electrons. The decay rate for the level correlated to the 6p level is also much affected by the presence of the L-band gap: in particular, at large Z, it is significantly lower on Cu(1 1 1) than on a jellium surface. At a very small distance from the surface, the energy of the '6p' level comes close to that of the Cu(1 1 1) $n = 1$ image state. The interaction between the localised '6p' state and the 2D image state continuum leads to an avoided crossing structure, that is not shown nor discussed here (see e.g., in Ref. [92] and below). The decay rate of this level will be discussed in more detail below.

At this stage, one can notice that, in the Cs/Cu(1 1 1) system at the adsorption distance, the states presented in Fig. 5 are well above the Fermi level in the case of a very small coverage. Their width is rather limited too, so that one can conclude that their population at equilibrium will be very small. The WPP study did not reveal any other quasi-stationary state that would be close to the Fermi level. These findings confirm the initial assumption of the calculation that the alkali core can be considered as an ionised one and that the excited states that are considered here in the low coverage limit correspond to the capture of an electron by the ionic Cs core. Indeed, the situation should change with coverage: an increasing coverage brings the adsorbate-localised states closer to the Fermi level (see e.g. Fig. 1).

The key point for the occurrence of long-lived states appears to be the quasi-blocking of the RCT in the Cs/Cu(1 1 1). This effect can be understood by looking at the resonant wave function that illustrates the characteristics of the excited state RCT decay on Cu(1 1 1) and on a free-electron metal (see also in Ref. [13,95,101]). Fig. 6 presents the square modulus of the resonant wave function for the lowest lying state (the one correlated at infinite Z to the 6s level of atomic Cs) in the case of Cs/Cu(1 1 1) and Cs/free-electron metal. z and ρ are the electron coordinates perpendicular and parallel to the surface. The Cs atom centre is located on the z-axis at the origin of coordinates. On Cu(1 1 1), the Cs atom is at the adsorption distance (3.5 a_0 from the image plane). For the free-electron case, the Cs adsorbate is located further away from the surface, at 10 a_0 from the image plane, in order to keep the decay rate of the state at a reasonably low value. The RCT process corresponds to the tunnelling of the active electron through the potential barrier separating the atomic well and the metal well. The transparency of the barrier is the highest along the surface normal that goes through the atom centre, since that is where it is the thinnest. So, a priori, one can expect the RCT to favour transitions along the surface normal, i.e., to preferentially populate metal states with a vanishing $k_{\|}$, electron momentum parallel to the surface. This is indeed the case in the free-electron case (Fig. 6b), where one can see that the outgoing electron flux of the excited state decay is centred on the surface normal. One can notice that the outgoing flux decreases rather rapidly as one moves away from the normal, indicating a very fast decrease of the barrier transparency with the emission angle. The picture is completely different in the Cu(1 1 1) case, due to the electronic structure of the

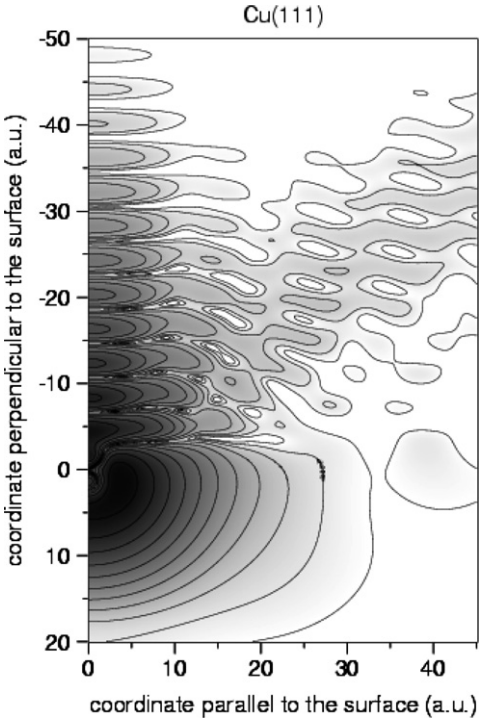

Fig. 6a. Wave-packet for the transient state in the Cs/Cu(1 1 1) system. It presents $\log(|\Psi|^2)$ in cylindrical coordinates: z, normal to the surface (positive in vacuum) and ρ, parallel to the surface. The dark areas correspond to large probabilities for the electron and the thin full lines to contour lines. The Cs atom center is at the origin of coordinates. The adsorbate–surface distance is 3.5 a_0 with respect to the image plane.

Cu(1 1 1) surface. This structure is schematically shown in Fig. 7, which presents the energy of the metal states as a function of $k_{\|}$. At $k_{\|} = 0$, the projected band gap lies between 5.83 eV and 0.69 eV below the vacuum. In the model used here (model potential from Ref. [97]), the position of the band gap is a parabolic function of $k_{\|}$, corresponding to the free electron mass. Inside the projected band gap, a surface state (SS) and image states (IS) are present (see e.g., in Ref. [25]). As discussed above, the RCT decay of the excited state is an energy conserving transition that should favour transitions to metal states around $k_{\|} = 0$. This is impossible on Cu(1 1 1), since there is not any $k_{\|} = 0$ Cu state in resonance with the Cs state energy (indicated by the horizontal line in Fig. 7). The only available metal states for the excited state decay correspond to large $k_{\|}$ in the surface state or in the 3D-propagating bulk band. Thus, the RCT decay can only populate large $k_{\|}$ states resulting in a drastic reduction of the RCT rate as compared with the free-electron case. This aspect is well illustrated in Fig. 6a. No outgoing flux is present along the surface normal. The largest outgoing flux corresponds to the population of 3D propagating bulk states; it appears beyond a certain angle from the surface, i.e., beyond a certain finite $k_{\|}$. In this system, very little population of the surface state occurs, due to polarisation effects (see a discussion in Ref. [95] and below). One can stress here that the model description of the Cu(1 1 1) surface [97] that is used in the present theoretical approach implies a free-electron motion parallel to the surface. With a more realistic band structure, the

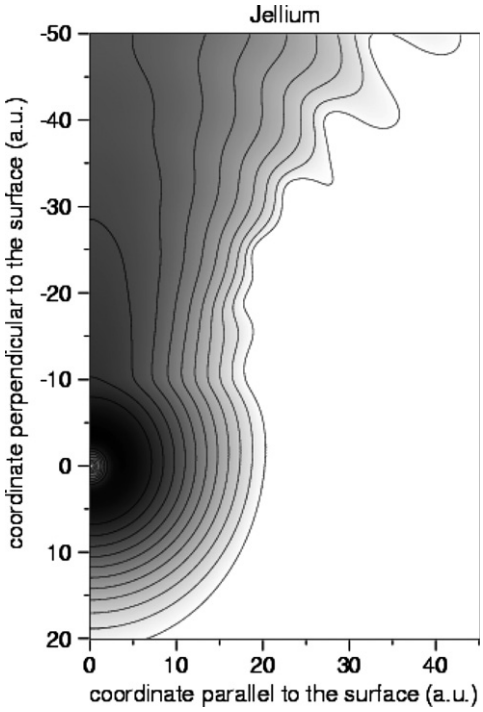

Fig. 6b. Wave-packet for the transient state in the Cs/free-electron metal surface system. It presents $\log(|\Psi|^2)$ in cylindrical coordinates: z, normal to the surface (positive in vacuum) and ρ, parallel to the surface. The dark areas correspond to large probabilities for the electron and the thin full lines to contour lines. The Cs atom center is at the origin of coordinates. The adsorbate–surface distance is 10 a_0 with respect to the image plane.

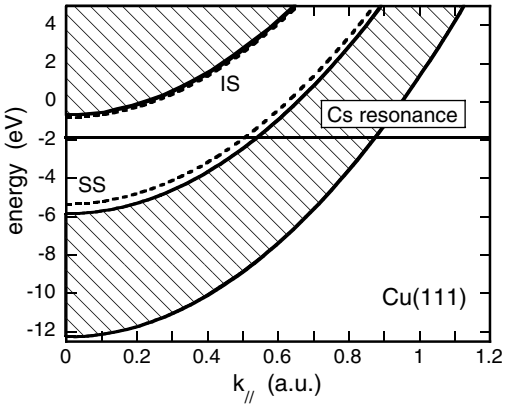

Fig. 7. Schematic electronic band structure of the Cs/Cu(1 1 1) surface obtained with the model potential from Ref. [97]: the energy of the electronic states in the model Cu(1 1 1) surface is given as a function of the electron momentum parallel to the surface ($k_{\|}$). Vacuum is at zero energy. The 3D propagating states are represented by the hatched area. The surface and first image states (dashed lines) are labelled SS and IS. The thick horizontal line indicates the Cu states degenerate with the Cs transient state.

Cu(1 1 1) band edges are not dispersing with a unit mass [25]. The minimum $k_{\|}$ required for a decay of the excited state would be smaller with a more realistic band structure, possibly affecting the RCT decay rates reported here.

Another feature is apparent on the Cs/Cu(1 1 1) wave packet picture. The resonant wave function is very different from the atomic 6s wave function it correlates to at infinite separation. In particular, it has lost its spherical symmetry. The Cs states thus appear to be much modified by the surface, even though the surface-induced decay is weak. Qualitatively, the main terms in the electron interaction with the surface are the interactions with its own image and with the ionic core image. Globally, the electron is repelled from the surface. Close to the surface, image charge interactions are large and are able to mix the various atomic levels, creating hybrids, similar to Stark states. The lowest lying level is correlated at infinity to the 6s atomic level. When the alkali–surface distance decreases to the adsorption distance range, the 6s level evolves into a hybrid that is mainly pointing away from the surface and that is formed from the 6s, 6p and higher lying levels. This is well apparent in Fig. 6a, where the resonant wave function appears to be pushed from the atom centre toward vacuum. This strong polarisation of the electronic cloud enhances the effect of the Cu projected band gap (see a discussion in Ref. [95]). In particular the sharp drop around 7 a_0 of Γ_{RCT} when the atom approaches the surface is attributed to the onset of the s–p mixing in the resonant wave function.

One can come back to the variation of the RCT decay rate of the level correlated with the 6p level at infinity (Fig. 5) and discuss it along the same lines as with the lowest lying state. Although this state does not remain a pure 6p state, for convenience we will still call it '6p' below. First, one can see that at very large Z, the difference between the RCT rates on a jellium and on Cu(1 1 1) is much larger for the '6p' state than for the '6s' state, even leading to an inversion of the relative values of the 6s and 6p decay rates. This is attributed to the different energy positions of the levels inside the L-band gap. The 6p level is higher in the gap than the 6s and thus its decay has to involve metal states with a larger $k_{\|}$, leading to a stronger blocking effect of the band gap. As Z decreases in Fig. 5, one notices around $Z = 9$ a_0 a sharp drop of the RCT decay rate of the '6p' state. It is attributed to the onset of the mixing between the 6p level and the higher lying 5d level. The slope change in the energy and width of the 6p level on a free-electron metal that occurs in the same Z range is similarly attributed to the onset of the p–d mixing. Closer to the surface, the rise of the 6p RCT rate on Cu(1 1 1) is interpreted as due to the onset of the mixing with the lowest lying s state. Indeed, the mixing that is responsible for the formation of a 'more stable' hybrid with a wave function pushed away toward vacuum is associated with the formation of a 'less stable' hybrid with its wave function pushed toward the metal. Precise assignment of the hybrid structure of the higher lying states is, however, more difficult than for the lowest lying one, due to the existence of the mixing of several atomic states corresponding to different orbital angular momenta, ℓ, but also to different principal quantum numbers, n. In this system, further complications arise since the 6p state comes close to the image state continua and to the upper edge of the L-band gap (see a discussion of these effects below in Section 5.1).

4. Aspects of excited state lifetime

In this section, a systematic review of the different aspects of the long-lived state in the alkali/noble metal systems as obtained from theoretical and experimental investigations is

given. In the first part, theoretical results obtained in a static approach, in which the adsorbate is kept at a fixed distance from the surface, are discussed in comparison with corresponding experimental results. This static approach applies to qualitative aspects of the excited state lifetime; it can also be quantitative provided the lifetime is not long enough to allow a significant motion of the adsorbate during the state lifetime. On longer time scales, electronic and nucleus degrees of freedom cannot be treated independently. Experimental results that clearly show the effects of the nuclear motion induced by the electronic excitation are presented in the second part of this section and a dynamical theoretical approach, taking the coupled electronic and nuclear motions into account, is described. This allows a discussion of the effect of nuclear motion on the electronic state characteristics.

Before we compare experimental and theoretical results, it is important to briefly discuss what to compare. As outlined above, time-resolved 2PPE allows, in principle, experimental access to the depopulation time T_1, to the total dephasing time T_2 and to the pure dephasing time T_2^* of an excited electronic state. These times correspond to the evolution of the excited electron when it interacts with the rest of the system. Different processes can occur due to these interactions. If they lead to a transition to another electronic state, they contribute to the depopulation time, T_1. If the interaction does not lead to a change of the electronic state, but simply to a phase-shift, like in an elastic scattering process, then it leads to the destruction of the coherence between the various electronic states and so it contributes to the pure dephasing time, T_2^*. Similarly, transitions between degenerate or quasi-degenerate states if not resolved experimentally also contribute to the pure dephasing time, T_2^*. Both pure dephasing and population decay contribute to the total dephasing time T_2 ($1/T_2 = 1/T_2* + 1/2T_1$). As described in Section 2.1, the model calculations consider resonant charge transfer (RCT) processes from adsorbate to substrate as well as multi-electron terms (inelastic electron–electron interaction). Both these processes lead to the decay of the population of the excited state. The theoretical values have, therefore, to be compared with the experimental value for T_1. Experimentally T_2 is accessible either by line-width measurements or by interferometric time-resolved two photon photo-emission (ITR2PPE). The strong inhomogeneous broadening of the alkali-induced resonances at elevated temperatures (see Section 2.1) restricts the measurement of the dephasing time in the frequency domain to low temperatures. Measurements of T_2 for Cs/Cu(1 1 1) by means of ITR2PPE have been performed for temperatures up to 300 K [12]. These measurements indicate only a weak temperature dependence of the total dephasing time T_2 of the excited alkali state and a value of about 10 fs. Compared to the measured depopulation times T_1 of (at least) 15 fs for Cs/Cu(1 1 1), this value shows that a significant contribution to T_2 is due to pure dephasing processes.

4.1. Static approach

4.1.1. Comparison between different surfaces: effect of the characteristics of the substrate band structure

Both the (1 1 1) and (1 0 0) surfaces of noble metals exhibit a projected band gap in the direction normal to the surface, however at different energy positions. In contrast, the (1 1 0) surface does not have a projected band gap along the surface normal. Table 2 presents experimental [10–12,79] and theoretical [101] results obtained for a Cs adsorbate on different noble metal surfaces, thus allowing an analysis of the effect of the substrate

Table 2
Characteristics of the adsorbate-induced quasi-stationary state in various Cs/noble metal systems

System	Cs/Cu(1 1 1)	Cs/Cu(1 0 0)	Cs/Ag(1 1 1)	Cs/Cu(1 1 0)
Energy (experimental)	3.1 eV	3.15 eV	2.7 eV	
Lifetime	50 fs at 33 K [12]	2.6 fs at 33 K [79]	30 fs at 33 K [79]	2.2 fs at 33 K [79]
(experimental)	15 ± 6 fs at 300 K [10]	6 ± 4 fs at 300 K [11]	>7 fs at 300 K [11]	
Energy (Theory [101])	2.99 eV	3.16 eV	–	–
Lifetime (Theory [101])	28 fs	5 fs	–	–

The energy of the state is given in eV with respect to the Fermi level and corresponds to the limit of very small adsorbate coverage on the surface. The lifetime is given in fs. There are two experimental sets corresponding to two different substrate temperatures.

characteristics. With the exception of the (1 1 0) surface, a long-lived state is experimentally observed in all cases, the Cu(1 1 1) case being the most spectacular. Note, however, that the lifetimes predicted and measured for Cs/Cu(1 0 0) and (1 1 0) are close to the limit of the time resolution of TR-2PPE. The experimental lifetimes appear to depend on the system temperature. A discussion of possible origins for the apparent temperature effect together with the effect of the adsorbate motion will be given below, in Section 3.2. As for the theoretical results [101], limited to the Cu surfaces, they do reproduce the large difference between the lifetimes on the (1 0 0) and (1 1 1) surfaces, the theoretical lifetime being typically in-between the experimental values at 33 K and 300 K. The differences between the lifetimes obtained in the (1 0 0) and (1 1 1) surface cases can be interpreted within the model presented above in Section 2.2 which predicts that the long lifetime is due to the quasi-blocking of the RCT in these systems. If one goes back to Fig. 7, which presents a schematic picture of the Cu(1 1 1) electronic band structure, one can see that the efficiency of the RCT is related to the energy position of the quasi-stationary state within the projected band gap. Indeed, the higher the resonant state in the band gap, the larger $k_{\|}$, the electron momentum parallel to the surface of the electrons transferred into the bulk, should be and the more reduced the RCT decay rate is. The projected band gap in Cu(1 0 0) is located at higher energies than that in Cu(1 1 1). The adsorbate-induced resonance is then closer to the band gap bottom in the Cu(1 0 0) case, so that the blocking effect is weaker. This leads to a very different RCT decay rate of the Cs-induced state on the two surfaces: 112 meV (Cu(1 0 0)) vs. 7 meV (Cu(1 1 1)). In contrast, the decay rate via inelastic electron–electron interaction determined within the many-body response theory approach appears to be much less sensitive to the characteristics of the substrate band structure. It is comparable on the Cu(1 0 0) and (1 1 1) surfaces (20 meV and 16.5 meV). Finally, the difference between the Cs/Cu(1 1 1) and (1 0 0) systems in Table 2 can be attributed to the RCT rate difference, induced by the different energy positions within the band gap. The position of the projected band gap of Ag(1 1 1) is close to the position of Cu(1 1 1), which is consistent with the long lifetime found in this system.

The (1 1 0) surface deserves some further comments. No projected band gap along the surface normal is present therefore one does not expect any stabilisation effect and the decay rate should be comparable to that found in the jellium case. On a jellium, the RCT decay of an alkali state is extremely fast [21,44,82,84], below 1 fs. At this point, one must go back to the interpretation of the population decay in the TR-2PPE experiments, where the photo-emitted electrons are detected along the surface normal. On Cu(1 1 1) and Cu(1 0 0), the RCT resonance decay populates states far from the surface

normal ($k_{\|} \gg 0$), which are not detected in an experiment looking at photoemission along the surface normal, so that the RCT decay is observed as a population decay. In contrast, on Cu(1 1 0), the resonance decay populates states around the surface normal ($k_{\|} \approx 0$) and these are observed together with the resonant state in a photoemission experiment looking along the surface normal. In this case, a real-time experiment probes both the dynamics of the RCT and the decay of the substrate state at the resonance energy. In particular, the long time behaviour of the photoemission will be dominated by the slower of these two processes. In other words, in the absence of a significant trapping of the electron around the adsorbate (very short lived adsorbate-induced state), the observed lifetime should be the same as on a clean surface; it is then equal to that of a hot substrate electron and not to the lifetime of the adsorbate-induced state.

4.1.2. Comparison between different alkalis: effect of the adsorbate characteristics

The different alkali atoms have a similar electronic structure and one can expect all of them to induce long-lived states when adsorbed on a noble metal similarly to Cs. Table 3 shows experimental [10–12,79] and theoretical [101,102] results for different alkali adsorbates on a Cu(1 1 1) surface. On the theoretical side, a long-lived state is always present with a clear evolution along the alkali series: the heavier the alkali, the longer the lifetime. The RCT and inelastic electron–electron interaction contributions exhibit the same variation along the series, however, the RCT rate presents the largest variation (a factor of 10 from Cs to Na) and it is thus the main origin of the variation of the state lifetime. Experimentally, the same evolution along the alkali series is observed, however with a very short lifetime in the Na case. Different features of the adsorbed alkalis can be invoked to account for this evolution along the alkali series. They have been discussed in detail in Ref. [102]. First, one could invoke the adsorption height, which is different in the three systems or the different energy positions of the resonance, which could lead to an effect similar to that discussed in Section 4.1.1. As shown in Ref. [102], these effects are too weak to account for the variation of the lifetime along the alkali series. One should then go back to Section 3.2.4, where the band gap effect as the origin of the long lifetime is discussed in

Table 3
Characteristics of the adsorbate-induced quasi-stationary state in various Alkali/Cu(1 1 1) systems

	Na/Cu(1 1 1)	K/Cu(1 1 1)	Rb/Cu(1 1 1)	Cs/Cu(1 1 1)
Theory [101,102]				
Adsorption height (measured from image plane)	2.5 a_0	3.4 a_0	3.6 a_0	3.5 a_0
Energy (Theoretical, with respect to Fermi level)	2.78 eV	2.74 eV	2.78 eV	2.97 eV
One-electron decay rate Γ_{RCT}	70 meV	16 meV	10 meV	7 meV
Inelastic electron–electron decay Γ_{ee}	22 meV	18 meV	17 meV	15 meV
Level lifetime $\tau = 1/(\Gamma_{RCT} + \Gamma_{ee})$	7 fs	19 fs	24 fs	30 fs
Experiments				
Level lifetime	1.6 fs (300 K) [79]		25 fs (33 K) [79]	15 ± 6fs (300 K [10,11]) 50 fs (33 K [12,79])

The energy of the state is given in eV with respect to the Fermi level and corresponds to the limit of very small adsorbate coverage on the surface. The lifetime is given in fs. There are two experimental sets corresponding to two different substrate temperatures.

detail. An important aspect is the polarisation of the excited orbital by its interaction with the surface, which repels the electronic cloud into vacuum. This clearly appears on the wave function in Fig. 6 and is responsible for the drop of Γ_{RCT}, when the adsorbate–surface distance decreases (see Fig. 5). The polarisation of the electronic cloud is very efficient in enhancing the band gap effect. The different free atomic alkalis have different polarisabilities [109]: 24.08, 43.4, 47.3 and 59.6 Å^3, for the Na, K, Rb and Cs. When interacting with a surface, their electronic cloud will then polarise in different ways. This effect is quite visible in Fig. 3 in Ref. [102], where the wave function of the excited state in the Cs case is seen to extend further into vacuum than in the Na case. This different polarisation of the electronic cloud combined with the band gap leads to a longer lifetime for the Cs case. The evolution of the excited state lifetime along the alkali series is then attributed to the evolution of the polarisability of the alkalis along this series. To further stress this relation, one can also mention the case of Li, for which a detailed study is not available. However, the RCT decay rate for a Li atom in front of Cu(1 1 1) has been reported as a function of the alkali–surface distance in Ref. [13]; at short atom–surface distance, it is very close to the RCT rate for Na consistently with its polarisability [109], 24.3 Å^3, which is very close to that of Na (24.08 Å^3).

4.1.3. Variation of the excited state characteristics with adsorbate coverage

In Fig. 1 we showed the coverage dependence of the various surface features in the Na/Cu(1 1 1) system. Increasing the coverage strongly influences the alkali-induced state. Its energy rapidly changes and the level comes closer to the Fermi level, shifting by as much as a couple of eV for a 0.2 ML coverage. Changing the surface coverage appears to be a possibility for tuning the resonance energy with respect to the substrate band structure. Following the above discussion, one may wonder about the effect of this energy shift, and more generally of the presence of alkali neighbours, on the excited state lifetime. Experiments at room temperature [11] (see Fig. 8) as well as low temperature [12] for

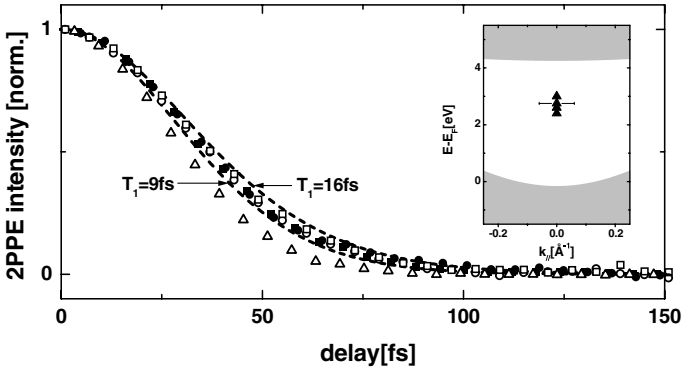

Fig. 8. Lifetime of the Cs resonance as a function of its position within the Cu(1 1 1) band gap at 300 K as probed by time-resolved 2PPE. The tuning of the resonance energy is easily performed by an increase in the cesium coverage. The inset shows the energy range of 0.6 eV probed within the experiment (black triangles correspond to the respective position of the cesium resonance). The experimental autocorrelation traces (solid and open squares and circles) show no significant difference indicating a resonance lifetime independent of the resonance energy. The dashed lines in the figure are results of the modelled autocorrelation traces for $T_1 = 9$ fs and $T_1 = 16$ fs. The open triangles correspond to the measured laser autocorrelation.

Cs/Cu(1 1 1) have been performed. In both cases, no detectable change in the measured lifetime could be found, although, in the data shown in Fig. 8, the energy of the cesium resonance varies between 3.0 eV and 2.4 eV (with respect to Fermi level, see inset of Fig. 8). Using the relation between the work function and the coverage [61], one can estimate the maximum coverage in Fig. 8 to be of the order of 0.1 ML corresponding to a density of 4.4×10^{13} cesium atoms/cm^2 (the saturation coverage for Cs on Cu(1 1 1) amounts to 0.25 the surface density of the Cu substrate [61]). From a theoretical point of view, two different types of effects can play a role in this coverage dependence: (i) the long-range interaction between the various adsorbates, dominated by the dipole associated to each adsorbate and (ii) the exchange interaction between adsorbates, corresponding to the possibility of a jump of the excited electron from one adsorbate to another. The interaction (ii) is of shorter range and can be thought to be ineffective for the relatively small coverages considered in Fig. 8. In contrast, the long-range action of all the other adsorbates on a given excited state plays a role.

The long-range effect of the neighbouring adsorbates has been modelled in the case of Cs/Cu(1 1 1) in Ref. [13]. It follows an earlier work (see e.g., Ref. [110–112] for details) in the context of the collisional charge transfer between a projectile and a surface with a small coverage of alkali adsorbates. The general idea is to explicitly treat a given Cs adsorbate, Ads_1, as outlined in Section 3.2, whereas all the other adsorbates are only represented by a long-range dipolar field. All the dipoles from the distant adsorbates are averaged into a dipolar plane, from which a disk is cut out to avoid double counting the adsorbate Ads_1. Such an approach is well adapted to the small to moderate adsorbate coverage before the occurrence of the depolarisation of the adsorbate layer. The corresponding results for the energy of the Cs-induced quasi-stationary state are presented in Fig. 9 together with the experimental results [10]. The results [13] are presented as a function of the surface work function change, $\Delta\Phi$, equivalently to a coverage scale. As can be seen, the modelling reproduces the energy variation observed experimentally quite well. One notices that the energy change of the excited state is smaller than the work function change

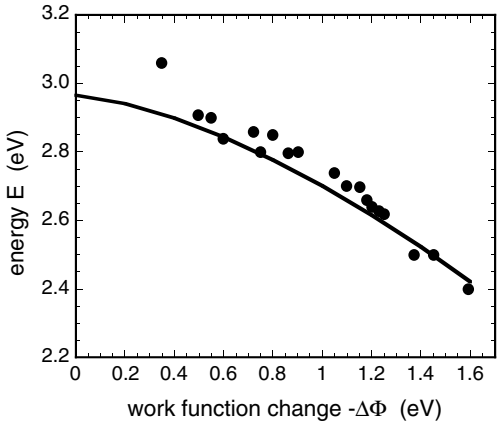

Fig. 9. Energy of the 6s resonance in the Cs/Cu(1 1 1) for various Cs coverage of the surface. The energy of the resonance is given with respect to the Fermi level as a function of the alkali adsorbate induced change of the surface work function. Full line: theoretical results [13]. Black dots: experimental results [10].

of the surface. This can be attributed to the fact that the excited electronic cloud lies above the surface image plane but does not penetrate deeply into vacuum and does not fully feel the potential change induced by the adsorbate dipoles. Following this idea, it is possible to show [13] that the variation of the energy of the excited state is roughly proportional to $(\Delta\Phi)^{3/2}$.

As for the RCT decay rate, it has been evaluated within the same modelling. The variation of Γ_{RCT} is small and non-monotonic at low coverage and becomes significant for larger coverages (see Fig. 4c in Ref. [13]). This variation has been attributed to the quasi-balance between two opposite effects [13]: on one side, the down-shift of the energy that moves the level down in the band gap and leads to a weakening of the band gap effect and on the other side, the increase due to the long-range dipolar potential of the barrier separating the adsorbate and the metal which results in a decrease of the barrier transmission. Nevertheless, Γ_{RCT} remains below 10 meV in most of the investigated coverage range. When varying the coverage, the lifetime of the excited state is not deeply affected by a change in Γ_{RCT}. The contribution of the electron–electron inelastic interactions in the excited state decay also has to be taken into account in the discussion of the lifetime variation. One could expect Γ_{ee} to decrease as a consequence of the level energy downshift, following Fermi liquid theory which predicts a variation of the rate proportional to $(E - E_F)^2$ (see e.g., in Ref. [23]). If we apply this scaling law to the energy change observed in Fig. 8, from 3 eV down to 2.4 eV, one gets a factor of 1.56 for the lifetime, which should be clearly observable in a TR-2PPE experiment. However, the effects mentioned above about the RCT rate also influence the wave function of the quasi-stationary state as well as those of the metal states and thus could affect the Γ_{ee} rate. In the absence of a detailed calculation of the dependence of Γ_{ee} on the coverage, it is difficult to further discuss this point, except by stressing that the Γ_{RCT} rate which is usually at the origin of the main variations and characteristics of the long-lived states (see above discussions) is only weakly dependent on the coverage in the low coverage range.

4.1.4. Relative role of the different decay channels

From the analysis presented above, one gets the relative importance of the various decay channels of the quasi-stationary states. Up to now, this information comes almost entirely from theoretical studies, with the exception of collisional studies discussed in Section 4.2.4. Γ_{ee} does not vary much from one system to another, whereas Γ_{RCT} presents large amplitude variations, so that the excited state decay is dominated by one or the other process, depending on the system. As a rule of thumb, the decay of the longer lived states (e.g., Cs/Cu(1 1 1)) is dominated by inelastic electron–electron interactions, whereas the decay of the shorter lived states (e.g., Cs/Cu(1 0 0) or Na/Cu(1 1 1)) is dominated by the RCT. It is possible to further analyze and look at the relative importance of the various substrate states in the RCT decay. Cu(1 1 1) exhibits a Shockley-type surface state close to the bottom of the projected band gap and RCT can populate both 3D-propagating bulk states and the surface state continuum (see Fig. 7). On Cu(1 0 0), only a surface resonance is present. Depending on the system, the relative importance of the RCT decay channels are very different. In Li–Cu(1 1 1) at large Li–surface distances, Z, the RCT decay for the state correlated at infinity to the Li(2s) atomic state is dominated by the surface state and Γ_{RCT} is, in this case, larger than on a free-electron metal [13]. This is attributed to (i) the difference between the normalisations in 2D and 3D that favours the surface state over the 3D-propagating bulk states and (ii) at large Z, the low energy position of the Li state

in the projected band gap where the blocking effect of the band gap is weak. The importance of the 2D surface state continuum can be related to other cases where the 2D continua (surface or image states) heavily contribute to surface processes [113–117]. In contrast, at small Z, in the Cs/Cu(1 1 1) case, transitions to the surface state are practically absent (see e.g., Fig. 6), due to the strong polarisation of the excited state wave function (see a discussion in Ref. [95]). In this system, the polarisation of the electronic cloud results in the narrowing of the range of $k_{\|}$ states populated by the RCT and to the appearance of a node in this distribution. An illustration of this polarisation effect can be found in Ref. [118] for the H/Al system. The node in the $k_{\|}$ spectrum suppresses transitions in a certain $k_{\|}$ domain, which, in the Cs/Cu(1 1 1) case, happens to be the range concerned with the surface state and therefore the contribution of the surface state to the decay is extremely small.

The relative importance of the surface state and 3D-propagating state contributions in RCT could also be modified by the variation of the alkali coverage. Indeed, as seen in Fig. 1, the energy of the Shockley surface state shifts down as coverage is increased, the state enters the 3D-propagating s–p band of Cu where it becomes a resonance and even eventually completely disappears. Similarly, in the Cs/Cu(1 1 1) case, in the 2PPE spectrum, we observed a downward shift of the Shockley surface state as the Cs coverage was increased. For a coverage of 0.15 ML, corresponding to a Cesium resonance energy of approximately 1.7 eV, no signal from the surface state at $k_{\|} = 0$ was detected [119]. In such a case, the RCT decay will only populate 3D states, although possible contributions from a surface resonance may be included. Similarly, a surface resonance is present on the Cu(1 0 0) surface and the RCT decay of alkali resonances, in this case, could also include contributions from the surface resonance imbedded in the contributions from 3D-propagating states.

No systematic experimental studies have yet been performed on this subject. At this point we refer to the outlook section where possible approaches to deconvolute the different contributions to the alkali decay in experiment will be discussed.

4.2. Dynamical approach

Electronic excitation of an adsorbate can induce an energy transfer between the electronic and the heavy particle motions that can lead to the adsorbate desorption. More generally, one can say that an electronic excitation of an adsorbate induces a change of the set of forces acting between the various components of the system. This phenomena can be described following the well-known 'Menzel–Gomer–Redhead' mechanism [120,121]. In this scheme, the adsorbate is initially in its electronic ground state at the adsorption equilibrium distance. If the adsorbate undergoes an electronic excitation, such as an electron capture or electron loss, the change of electronic state results in a change of the interaction potential between the adsorbate and the substrate; in particular, the adsorbate is not located at a minimum of this new interaction potential and it starts to move either toward or away from the surface. These new forces acting on the adsorbate only last for a finite time, given by the lifetime of the excited electronic state. The outcome of this mechanism depends on a few parameters: the electron to nuclei energy transfer is favoured by a steep potential energy curve of the excited state and especially by a long excited state lifetime. If the energy transfer to the adsorbate motion is large enough, desorption occurs; else, the electronic excitation only results in the excitation of the adsorbate vibrational motion in

the adsorption well. In the latter case, desorption could nevertheless occur via multiple successive electronic excitation. In the alkali-noble metal system, the excited state lifetime is quite long and indeed, a significant motion of the adsorbate can occur during the state lifetime. This effect is discussed below, together with a short account of the role played by the long-lived quasi-stationary states in collisional charge transfer.

4.2.1. Motion of the Cs adsorbate induced by photo-excitation in Cs/Cu(1 1 1)

The TR-2PPE in the fs domain allows one to follow the time evolution of a system with a pump–probe method. Using this approach, Petek et al. [79,122] have very clearly demonstrated the existence of nuclear motion during the lifetime of the lowest excited state in Cs/Cu(1 1 1). Their results [79] are presented in Fig. 10 and show the differential two-photon photoemission spectrum as a function of the emitted electron energy for different time delays between the pump and probe pulses. In the zero delay spectrum, two components appear corresponding to the non-resonant 2PPE of the Cu(1 1 1) surface state (around 5.8 eV) and to the 2PPE via the Cs-induced excited state (around 6 eV). When the time delay increases, the non-resonant peak disappears while the resonant peak shifts in energy, bringing direct evidence for the evolution of the excited state during its lifetime.

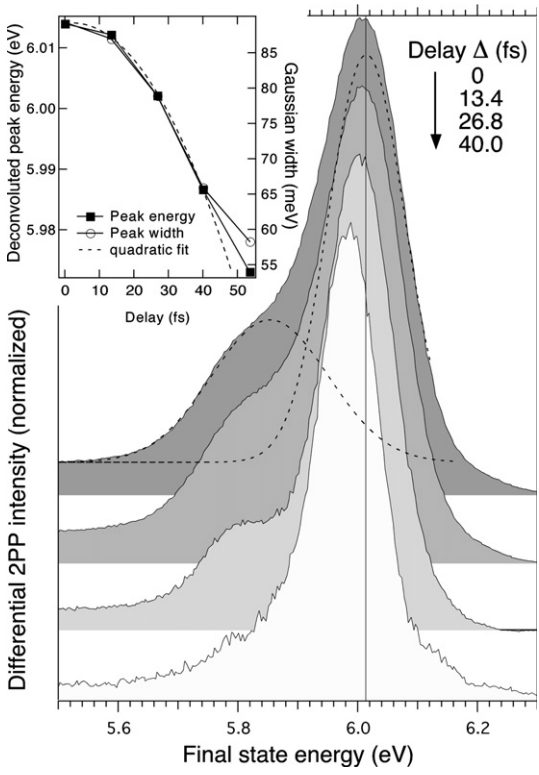

Fig. 10. Two-photon photoemission difference spectra taken at 13.4 fs intervals. Dashed lines: deconvolution of the surface state and alkali resonant state contributions. Vertical full line: position of the alkali resonant state at zero delay. The inset shows the deconvoluted peak energy and width as a function of the time delay (Reprinted with permission from reference [79]. Copyright (2000) American Chemical Society).

The evolution revealed in Fig. 10 can be understood from Fig. 5, which shows the energy of the excited state as a function of Z, the Cs–Cu distance. If the interaction potential between the excited adsorbate and the substrate is assumed to be the sum of the interaction potential of the Cs^+–Cu system (ground state) and of the energy of the excited electron in the excited state (Fig. 5), this excited potential is very repulsive and thus the formation of the excited state leads to a stretching of the Cs–Cu distance, i.e., to a movement toward desorption. Since the energy of the excited state decreases when the Cs–Cu distance increases, the Cs motion induced by the photo-excitation results in a down shift of the photoemission line, as seen in Fig. 10. In addition, one could expect Cs desorption to take place. Petek et al. [79,122] have indirectly confirmed the existence of a photo-induced desorption induced via the long-lived excited state. The change of the surface work function induced by the photo-desorption has been used to get an upper limit of the photo-desorption cross section equal to 2.4×10^{-13} cm^2. This value is much lower than the one reported for a similar process in the K/Graphite system [123]. The difference has been attributed in Ref. [79,122] to the mass difference of the desorbing particles which does not favor Cs. Another very likely possibility is that the desorption energetic in Cs/Cu(1 1 1) is much less favourable than in K/Graphite. Desorption only occurs if the energy change of the excited electron from the adsorption distance to infinity is larger than the adsorption energy. In Cs/Cu(1 1 1), the electron energy change is around 1.9 eV equal to the adsorption energy of Cs as estimated in Ref. [79]. In that case, the photo-induced motion leads to a significant excitation of the Cs–Cu vibration, but to a very low desorption probability.

The time evolution of the excited electron in the Cs-induced state created by the first photon absorption in a TR-2PPE experiment has been modelled theoretically using a WPP approach [124]. The idea was to solve the WPP problem for the electron evolution with a time dependent Hamiltonian $H(t)$, where the t-dependence comes from the desorption motion of the classically treated Cs nucleus. The potential for the excited state desorption is modelled from the energy of the electronic level associated to the Cs(6s) level (Fig. 5) and from a harmonic potential [125,126] for the ground state. The initial state of the propagation is taken as the excited state at the adsorption equilibrium position. It mimics the population of the excited state by a 'pump' laser pulse at a delay time $\Delta = 0$ (the first photon of a 2PPE experiment). The electronic wave-packet is then propagated while the Cs–Cu distance varies according to classical dynamics. After a certain delay, Δ, a probe laser pulse acts on the electronic wave-packet and induces electron emission. In a sense, this pulse mimics the second photon of a TR-2PPE experiment. The probe pulse allows the analysis of the evolution of the system with time, namely to get the time dependence of the energy spectrum of emitted electrons. As a first result, Fig. 11 shows the position of the maximum of the emitted electron energy spectrum as a function of the delay, Δ. This quantity is directly comparable to the experimental observation. The agreement observed in Fig. 11 is quite satisfying, taking into account the approximations involved in the treatment of the heavy particle motion. It confirms the picture used to describe the process as well as the relevance of the modelling. It also confirms that the time evolution of the excited electron is adiabatic, i.e., that, during the desorption, the electron evolution corresponds to that of a single excited state decaying by electron transfer to the metal without any significant non-adiabatic transitions. In other words, this evolution could be described via a local complex potential approximation [14]. One can also quantify the magnitude of the desorption motion: during the first 100 fs, i.e., around 3 times the state lifetime, the state energy varies by 0.15 eV corresponding to a 0.4 a_0 Cs displacement.

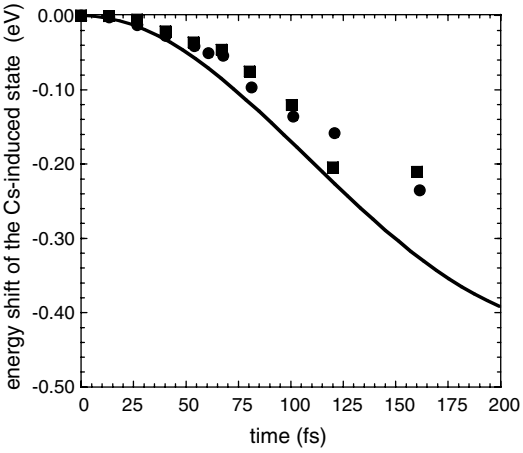

Fig. 11. Cs adsorbate movement induced by the excitation of the Cs(6s) resonance in the Cs/Cu(1 1 1) system. The figure presents the energy shift of the Cs(6s) resonance as a function of the time delay between the excitation of the resonance and its probe in a time resolved two-photon photoemission experiment. Symbols: two sets of experimental points from reference [122]. Full line: theoretical results from reference [124].

A rough estimate of the adsorbate displacement, useful to stress the various parameters influencing it, can be obtained from the classical motion of an adsorbate of mass, M, which is initially at rest and feels the action of an applied force $\mathrm{d}V/\mathrm{d}Z$ during a time T (T is typically equal to a few times the resonance lifetime). One thus gets a displacement of the adsorbate with respect to the surface, ΔZ, equal to:

$$\Delta Z = \frac{1}{2}\frac{\mathrm{d}V}{\mathrm{d}Z}\frac{T^2}{M} \tag{8}$$

This stresses the importance of a long-lived resonance to get a significant motion of the adsorbate.

4.2.2. Influence of the Cs motion on the photoemission spectrum

During the desorption motion, the spectrum of photoemitted electrons changes, as clearly evidenced in the experimental results [79,122]. Particularly the dependence of the photoemission on the time delay between the two pulses does not exhibit an exponential decrease, as it would if the only feature influencing the time-dependence were the excited state lifetime. Indeed, the time-dependence of the signal comes from a few factors: the exponential decay of the quasi-stationary state population, the change of the quasi-stationary state energy and lifetime with time and the resolution of the experimental observation window. The non-exponential behaviour is illustrated in Fig. 12 (from Ref. [124]) which presents the results of the modelling for the intensity of the photoemission spectrum at different energies, as a function of the delay, Δ. The energy of the emitted electron is referred to the energy corresponding to the Cs resonance at the Cs adsorption equilibrium distance. Except for the absence of a non-resonant contribution at very small Δ, the results shown in Fig. 12 are very similar to the experimental observations of Petek et al. [79,122]. Two very different behaviours can be observed. For an emitted electron energy corresponding to the centre of the emission line at the equilibrium position

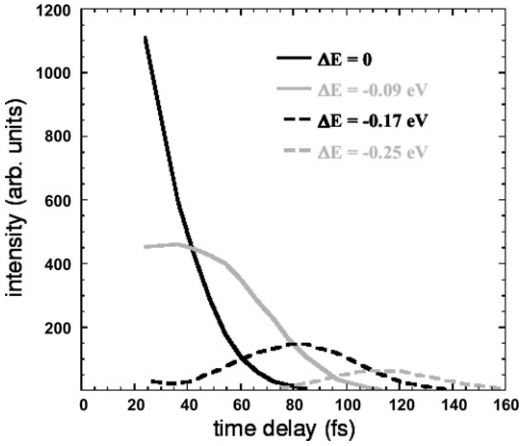

Fig. 12. Cs adsorbate movement induced by the excitation of the Cs(6s) resonance in the Cs/Cu(1 1 1) system. The figure presents the intensity of photoemitted electrons at different energies as a function of the time delay between the pump and probe laser pulses in a time-resolved two-photon photoemission experiment. The energy of the photoemitted electron, ΔE, is given with respect to the centre of the Cs(6s) line in the absence of Cs motion for a Cs adsorbate at its equilibrium position. (from Ref. [124]).

($\Delta E = 0$ eV), the signal decreases rapidly with time, faster than according to the state lifetime. In fact, the decay of the signal at $\Delta E = 0$ eV is due to two factors: (i) the decay of the population of the excited state and (ii) the down shift of the energy of the excited state with time (see Fig. 5). Because of (ii), the emission line which initially is centred at 0 is also shifting down in energy with time and moves out of the detection window. In the present calculation, the width of the detection window is given by the laser pulse duration. The behaviour at $\Delta E = -0.25$ eV is very different: basically no signal for small Δ and a peak around 120 fs. This corresponds to the fact that at $t = 0$, the emission line is centred on $\Delta E = 0$, so that the emission at $\Delta E = -0.25$ eV is very weak. However, later the Cs motion has shifted down the emission line, bringing it into the detection window. Emission at -0.25 eV only exists because of the Cs motion.

The Cs motion has a few other consequences. First, one must mention that the distribution of different adsorption distances in the initial state leads, via the distance dependence of the resonance line, to a strong inhomogeneous broadening of the photoemission lines. The spread in the alkali–Cu distance due to thermal population of the various vibrational levels gives an estimate of the inhomogeneous broadening at room temperature equal to 200 meV for Cs/Cu(1 1 1) and 320 meV for Na/Cu(1 1 1) [124]. This is a very significant contribution to the room temperature line widths shown in Table 1. This inhomogeneous broadening is much smaller when the temperature goes down, consistent with the narrowing of the photoemission lines observed experimentally (see Table 1 and Ref. [12]). The broadening of the photoemission line due to the Cs motion is much smaller (see Fig. 10) than the inhomogeneous broadening at room temperature. However, for low temperatures it can significantly contribute to the total line broadening. Another broadening mechanism in this system is due to the random character of the distribution of the alkali atoms on the surface. At low coverage, the alkali adsorbates are ionised and repel each other, however, their distribution on the surface is not perfectly inhomogeneous leading to an inhomogeneous broadening of the potential around a given adsorbate. This effect

has been investigated using a molecular dynamics approach [127] in the Na and Cs/Cu(1 1 1) systems. It leads to a significant broadening which increases with temperature, though the distribution of alkali adsorption heights appears as the dominant broadening mechanism.

Another important consequence of the Cs motion for the experimental analysis follows from the non-exponential behaviour of the time-dependence of the photoemission signal. The extraction of the quasi-stationary state lifetime from behaviours like those shown in Fig. 12 is not straightforward, as opposed to the case where no adsorbate motion is present and where the emission time dependence is a simple decreasing exponential. In principle, the lifetime extraction should involve a modelling of all the effects influencing the time dependence (decay of the state, Cs motion and experimental window). Fig. 12 shows data that correspond to the situation where the Cs is initially at rest in its equilibrium position; it should represent the situation of a very low temperature where only the ground vibrational level for Cs–Cu motion is populated. By contrast, at room temperature, the broadening referred to above should blur the effect of the Cs motion, restoring an almost exponential behaviour for a global averaged signal and allowing the extraction of an average lifetime for the quasi-stationary state. This effect is a likely origin for the apparent temperature dependence of the quasi-stationary state lifetime (see Table 1), since the fitting procedure that was used to extract the excited state lifetime from the experimental data ignored the effect of the adsorbate motion.

4.2.3. Computation of the photo-emission signal

As explained above, a direct extraction of the transient alkali state lifetime from the TR-2PPE signal is not straightforward due to the alkali motion, making a detailed quantitative comparison with the theoretical lifetime difficult. Such a comparison is more easily performed on an experimentally observable quantity. Recently, the time-dependence of the TR-2PPE signal in the case of Cs/Cu(1 1 1) has been computed using the theoretical description of the system discussed above [128]. Basically, it describes the system during the TR-2PPE experiment by a wave function product of a nuclear and an electronic part and it explicitly takes the two laser pulses into account. The calculation includes various initial and final states and an energy window is defined to select the experimentally measured final states. This allows one to compute the TR-2PPE signal and the energy spectrum of the ejected electron as functions of the time delay between the two laser pulses. Fig. 13 presents the corresponding results (slow component of the TR-2PPE signal) as compared to experimental results [129] obtained at room temperature with two different lasers of pulse duration 25 and 40 fs. Since the actual shapes of the experimental laser pulses are not accurately known, the calculations were performed with two shapes: Gaussian and hyperbolic secant. The agreement between the theoretical and the experimental results is quite satisfying. In fact the agreement between the computed signal and the raw experimental data are much better than the one between the computed lifetime and the one extracted from experiment, i.e., after some processing of the experimental data (see Table 2). One can stress that the theoretical signal is obtained using the theoretical lifetime in Table 2. The key point here is that the effect of the Cs motion is taken into account in the comparison.

In an interferometric TR-2PPE experiment, the photoemission signal can be split in three components: a slow varying component, one at the laser frequency and one at twice the laser frequency (see e.g., in [88]). Analysis of the three computed components

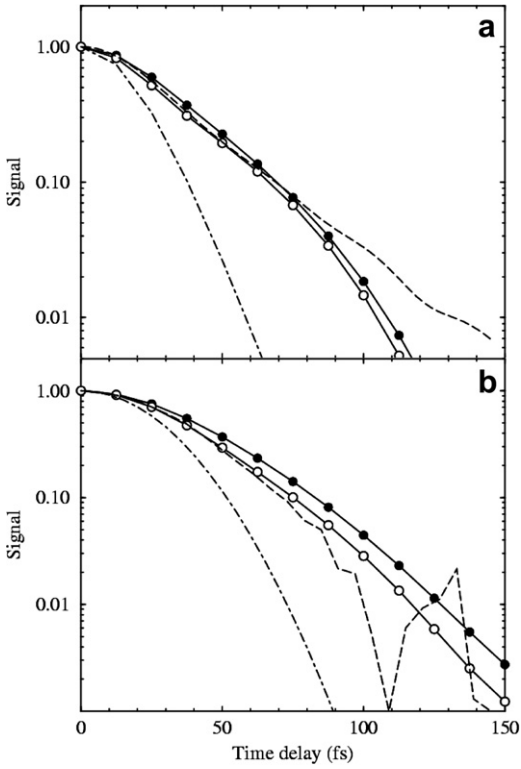

Fig. 13. Slow varying component of the TR-2PPE signal as a function of the time delay between the two laser pulses in the Cs/Cu(1 1 1) system. Comparison between experimental [129] and theoretical [128] 2PPE signals for a 25 fs (panel a) and 40fs (panel b) laser pulse duration. Dashed line: experimental data [129]. Full line with full circles: theoretical signal [128] for the 'sech' pulse shape. Full line with open circles: theoretical signal [128] for the gaussian pulse shape. Dashed dotted line: autocorrelation function of the 'sech' pulse shape.

elucidates the role of the various features of the system in the population and coherence evolution. As discussed above, the decrease of the TR-2PPE signal with time is due to the decay of the Cs^* state, to coherence decay and to the fact that the Cs^* state moves out of the detection window. One must stress that the approach in [128] that involves wave functions, does not introduce any pure dephasing process associated to the time T_2^*. This is at variance with the phenomenological description based on the optical Bloch equations (see the discussion above). Nevertheless dephasing processes are present in this system. It appears that the coherence between the initial state and the final photo-emitted electron state disappears very quickly when a summation is performed over initial and final states. More interestingly, the desorption motion of the Cs atom results in the time variation of its energy and thus to its dephasing since the quantal phase of the state, $\exp(-\mathrm{i}\int_t^{t+\Delta t} E(t')\,\mathrm{d}t')$, departs from a simple exponential $\exp(-\mathrm{i}\,E\Delta t)$. This interpretation is quite different from the usual one, in which dephasing is introduced via phenomenological terms in Bloch equations and is usually assumed to correspond to the interaction of the system with a heat bath. In Ref. [128], effective decay and dephasing times (T_1 and T_2) have been extracted from the theoretical photo-emission signals, assuming that the

various components in the signal can be described as convolutions of autocorrelations of the laser pulse with decreasing exponential [88]. These effective times compare well with the corresponding experimental data at room temperature [129]. This confirms (i) the variation of the effective times with the laser characteristics as observed by Bauer et al. [129] and (ii) that the effective Cs^* lifetime that can be extracted from the photoemission signal is significantly shorter than the real lifetime. In addition, the effective pure dephasing time T_2^* is found to be very close to the one that has been extracted from experiment [12], supporting the interpretation of the dephasing process in this system as mainly a simple consequence of the Cs motion.

4.2.4. Collisional charge transfer

The unoccupied quasi-stationary states observed by 2PPE also act as intermediates in the electronic processes occurring during the scattering of alkali projectiles from metal surfaces. In particular those are the states formed by the electron capture/loss processes at surfaces. In the case of collisions on clean free-electron metal surfaces, the electron transfer problem has been extensively studied [14] and accurate quantitative descriptions are now available [20,21]. Scattering from the (1 1 1) and (1 0 0) surfaces of noble metals reveal a few special characteristics that are linked to the features discussed above. First, the RCT rate, that governs the electron capture and loss processes in the course of an atom(ion) collision on a surface, can be significantly decreased due to the projected band gap. However, the band gap blocking effect has a strong dynamical aspect, i.e., it shows a pronounced dependence on the collision velocity. Indeed, it has been shown that the blocking of the RCT by the projected band gap can only be effective for a long enough interaction time. In a fast collision, the system probes the surface on a short time scale and the active electron does not have enough time to explore the target surface band structure [130]. The metal surface then behaves roughly like a free-electron metal. This aspect has been used to interpret experiments on the velocity dependence of the electron capture process during collisions [131,132].

Another effect of the (1 1 1) surfaces is due to the role played by the surface state in the collisional charge transfer. In the case of fast collisions in grazing angle geometry, the large velocity component parallel to the surface leads to the so-called parallel velocity assisted electron transfer process [14,133,134]. The two-dimensional character of the surface state leads to qualitative changes in this process which have been observed and theoretically accounted for in a few systems including H^- formation and alkali positive ions neutralisation in grazing scattering from Cu(1 1 1) surfaces [91,135].

5. Outlook and conclusions

In this section, we discuss a few extra features of the long-lived excited states on the alkali-noble metal systems that are currently under study, as well as extensions of these studies to other systems, where long-lived states have been observed or can be expected.

5.1. Search for other excited states in alkali/Cu systems

In the previous sections, we concentrated on the lowest lying excited state of the alkali/noble metal systems, this excited state is correlated at infinite separation to the ground state of the free alkali atom. One may also wonder about the existence of other higher

lying states and their possible long lifetimes. Until now, none have been experimentally observed. A theoretical study of these has been reported for the Cs/Cu(1 0 0) system [136].

First, one can look at the states correlated at infinite separation to the excited states of the alkali spectrum and see what is their lifetime at the adsorption distance. Going back to Fig. 5, one can see that the 6p ($m = 0$) state of Cs exists at a large distance from the Cu(1 1 1) surface with a small width, but that its decay rate becomes very large at small alkali–Cu distances, most likely making it very difficult to observe. As explained in Section 3.2.4, polarisation of the electronic cloud leads to an increase of the lifetime for the lowest state but also leads to a shortening of the lifetime of higher lying states. One can then expect shorter lifetimes for the higher states. The idea is to then look for long-lived states in other symmetries, where the lowest lying state of each symmetry should be in the best situation with respect to a long lifetime. The theoretical study of the Cs/Cu(1 0 0) system [136] has shown that an excited state of $m = 1$ symmetry is present roughly 0.5 eV above the well-known $m = 0$ state, with a comparable lifetime (7 fs against 5 fs). From this result, one can then expect such a long-lived state in each symmetry, as long as it does not interfere too much with image state continua (see below) and remains within the substrate projected band gap. The wave function associated to the $m = 1$ quasi-stationary state in Cs/Cu(1 0 0) [136] has a well-marked atomic character, however, it is strongly perturbed from the 6p ($m = 1$) atomic state it correlates to at infinity. As further proof of the strong modifications of these atomic-like resonances from their free-atom origin, one may notice that the energy distance between the two states in Cs/Cu(1 0 0), 0.5 eV, is much smaller than the corresponding 6s-6p energy difference in the free atom, that amounts to 1.44 eV. Calculations on the Cs/Cu(1 1 1) system also revealed the existence of a long-lived adsorbate-induced state in the $m = 1$ symmetry [137]. At the adsorption distance of 3.5 a_0, in the case of a single adsorbate on the surface, this state was found to be bound by 1.154 eV with respect to the vacuum level, 0.8 eV higher than the well-documented $m = 0$ state and inside the Cu(1 1 1) surface projected band gap. The decay rate of this $m = 1$ state was calculated to be 72 meV, corresponding to a 9 fs lifetime.

The study of the Cs/Cu(1 0 0) system revealed the existence of other states of a different type, with an energy slightly below the bottom of each of the 2D-image state continua [136]. These states were first revealed by the structures they induce in the scattering of image state electrons by individual alkalis on a Cu surface [138,139]. The appearance of these excited states has been related to the existence theorem for bound states in 2D by B.Simon [140]. Broadly speaking, this theorem states that, in 2D, any attractive potential should induce a bound state. The present situation is slightly different since the 2D-image state is imbedded in a 3D-continuum of bulk states. Nevertheless, the perturbation of a 2D-image state continuum by the attractive potential around an alkali adsorbate induces a localised state just below the image state bottom. The wave-functions of these extra states look like what one expects for a bound state in the 2D-image state continuum [136]. Because of the 3D character of the complete problem, these extra states have a finite lifetime and appear as resonances decaying into the 3D-continua or into lower lying 2D-continua. The lifetimes of these resonances are rather long, they range between 10 and 100 fs for the states in the $m = 0$ and $m = 1$ symmetries located below the $n = 1$ and 2 image states [136] (see Table 4). Such a long lifetime is a favourable characteristic for experimental observation. However, the energies of these 'split-off' states are very close to the bottom of the parent image state continuum. This might make them very difficult to observe, except for in experiments in which, $k_{\|}$, the electron momentum parallel to

Table 4
Energy (in eV with respect to vacuum), decay rates (in meV) and lifetimes (in fs) of the localised levels in the Cs/Cu(100) system in the $m = 0$ and $m = 1$ symmetries (m is the projection of electron angular momentum on the normal to the surface going through the alkali centre)

Symmetry	Energy (in eV)	RCT decay rate (in meV)	Total decay rate (in meV)	Lifetime (in fs)
$m = 0$	−1.46	115	134	5
$m = 0$	−0.609	5.2	13.6	48
$m = 0$	−0.224	54	56	12
$m = 1$	−0.926	77.4	88.3	7
$m = 1$	−0.574	2.3	10.6	62
$m = 1$	−0.203	4.1	6.7	98

In each symmetry, the first level is atomic-like, while the two others are respectively located just below the $n = 1$ and $n = 2$ image state thresholds. On Cu(100), the two first image state thresholds are located at −0.573 eV and −0.177 eV (with respect to vacuum).

the surface is resolved. One can stress that similar states have been observed by Photoemission, Inverse Photoemission and Scanning Tunnelling Microscope in the cases of image states perturbed by steps on a surface [141–144]. In that case, the attractive 1D-potential created by steps induces a 1D-state with an energy just below the image state bottom. It is associated with electron propagation along the step direction and is localised along the direction perpendicular to the steps. One can also mention that similar quasi-stationary states can also appear below the bottom of an existing surface state continuum [145,146]. These states could account for the structures observed with a scanning tunnelling microscope (STM) in the spectroscopic mode in various systems [147,148] and have been clearly identified in the Cu/Cu(111) system [146,149]. Theoretical studies of groups of several adatoms on a surface also reported quasi-stationary states induced by localisation of the 2D-surface state continuum [150].

Finally, it is worth noting that the two kinds of excited states mentioned above, atomic-like and split off from the 2D continua mix together when their energies are close to each other, making a clear assignment of their characteristics difficult. This feature can be very easily seen in theoretical studies in which the adsorbate–surface distance is changed. It allows for a change of the energy difference between the various states or, equivalently, allows to bring an atomic-like state close to the bottom of a 2D-continuum band. This can be found in Ref. [92], for the H^-–Cu(111) system, where the affinity level of hydrogen presents an avoided crossing with a state localised slightly below the bottom of the 2D-surface state continuum.

One can also stress the role played by the quasi-stationary states in the scattering of image state electrons by impurities at surfaces, where these states appear as scattering resonances. An image state electron can be seen as an electron travelling parallel to the surface and occasionally hitting the impurities that lie on the surface. Scattering of the image state electron by an impurity into another electronic band is associated with a population decay of the image states whereas, scattering inside the image state continuum results in a loss of coherence, i.e., a pure dephasing process for the electron. Both population decay and pure dephasing contribute to the broadening of the image state [138,139]. These two kinds of processes correspond to the electron either changing its direction of propagation while still travelling parallel to the surface (pure dephasing) or suffering a 3D-scattering event (population decay). Population decay and broadening of the image states

induced by adsorbates have been experimentally observed in a few systems, following pioneering work by Kevan [68,151–155]. In the limit of very low adsorbate coverage, the level lifetime and photoemission line widths vary linearly with the adsorbate coverage on the surface. Theoretical studies of electron scattering in the image state continua [138,139] show that quasi-stationary states play an important role as intermediates in this scattering, the cross sections as functions of the electron travelling energy present structures at the position of the quasi-stationary states mentioned above.

5.2. Other adsorbate/metal systems

In the above sections, we reviewed results on the alkali/noble metal systems which all present a long-lived quasi-stationary state. In this section, we will now look for long-lived states in other systems, progressively increasing the qualitative distance from the model 'alkali/Cu' system. This improves the discussion of the conditions for the observation of a long-lived excited state in a given adsorbate/substrate system.

5.2.1. Core excited Ar atoms on Cu surfaces

In discussions of atomic states with a core hole, the so-called $(Z+1)$ approximation is very often invoked [156,157], in which it is assumed that the spectrum of an atom with an electron missing in one of its inner shells is identical to that of the next atom in the periodic table. As an example, the core-excited Ar atom, $Ar^*(2p_{3/2}^{-1}4s)$, should look very much like a K(4s) state. Thus, one should expect that such a core-excited atom when adsorbed on e.g., Cu(1 1 1) would undergo the same RCT blocking effect as a K atom. A core excited $Ar^*(2p_{3/2}^{-1}4s)$ atom has two decay channels when adsorbed on a metal surface: (i) the RCT decay of the 4s electron into the metal (analogous to the decay of the K(4s) electron), followed by the Auger decay of the hole in the $Ar^+(2p_{3/2}^{-1})$ ion and (ii) the Auger relaxation of the core hole with the 4s electron as a spectator. Each of the two Auger decays produces a characteristic energy spectrum of ejected electrons, so that it is possible to separate the contributions from the two decay channels experimentally. This Resonant Auger Raman Spectroscopy [158,159] has been applied to a few Ar/metal systems [160–163]. If one assumes that the Auger decay of the 2p hole in Ar is not disturbed by the surface, and therefore the corresponding decay rate is the same as in the free atom, then the decay rate of the 4s electron can be obtained from the branching ratio of the two decay channels. With this method the decay of the core hole is used as a clock to measure the very fast transfer of the 4s electron into the metal substrate. Using this 'core hole clock method' it is thus possible to indirectly investigate the 4s lifetime when it does not greatly differ from the 2p hole lifetime.

Experimental results on the $Ar^*(2p_{3/2}^{-1}4s)$ state in the 1ML Ar/Cu(1 1 1) and Ag(1 1 1) systems have been reported recently [163]. The 4s electron energy lies within the Cu(1 1 1) and Ag(1 1 1) projected band gaps and its lifetime was found to be around 7 fs in these two systems, i.e., significantly longer than expected for a free-electron metal (around 1 fs). This confirms the RCT blocking role of the Cu(1 1 1) and Ag(1 1 1) projected band gaps. This lifetime is shorter than the lifetime of 19 fs reported in the analogous K/Cu(1 1 1) [102] system (see Table 3). A very recent theoretical study of the $Ar^*(2p_{3/2}^{-1}4s)$ state in the 1ML Ar/Cu(1 1 1) system [164] provided a lifetime around 12 fs, again confirming the very important role of the projected band gap in Cu(1 1 1). The effects of the presence of Ar neighbours in the Ar mono-layer as well as of the adsorption distance were also

found to significantly influence the level lifetime [164] and partly account for the quantitative differences found between the K(4s) and $Ar^*(2p_{3/2}^{-1}4s)$ systems. However, the theoretical study of K(4s) and $Ar^*(2p_{3/2}^{-1}4s)$ single adsorbates at the same adsorption distance leads to different lifetimes [164], so that the $(Z+1)$ approximation is not fully accurate in this case. Experimental studies with other metal substrates [161,162] (Ru(0 0 1), Ag(1 1 0), Au(1 1 0), Cu(1 0 0) and Pt(1 1 1)) reported 4s lifetimes in the 1-5 fs range (the longer was on Pt(1 1 1)), the differences being tentatively attributed to the different band structures of the substrates.

5.2.2. Alkalis on other substrates

The above discussion focused on alkali adsorption on noble metal surfaces. It was found that for these systems the localisation of the alkali resonance within the sp band-gap is essential for the existence of a long-lived excited state. In the case of a free-electron metal surface where there is not any projected band gap, theoretical studies predict very short-lived excited states for the alkali adsorbates (see discussions in Sections 2.2 and 3.2.4). The sp band gap is also present in transition metals, however, the situation is more complex because – in contrast to noble metals – the d-bands overlap the Fermi edge and can be close to the adsorbate induced level. Depending on their energy with respect to an adsorbate resonance, these d states will mix with the adsorbate levels and influence both the RCT and the electron–electron inelastic interactions. Due to high chemical activity, transition metals are interesting systems for the study of the charge transfer process and its connections with chemical surface reactions. In search of a transition metal substrate that exhibits a long-lived alkali excitation, one could look for band structure conditions as close to the noble metal case as possible. Excited alkali states at transition metals have been observed for the systems K/Fe(1 1 0), Na/Fe(1 1 0) and Na/Co(0 0 0 1) by Fischer et al. by means of 2PPE [66]. The coverage dependence of the investigated state is similar to the results obtained for the Na/Cu(1 1 1) system (see Fig. 1) indicating that the corresponding unoccupied ns-levels of the alkali are observed. Real-time studies for these systems have not been published so far. However, in connection with time-resolved 2PPE studies of bulk excitation of thin films of Co, Ni and Fe [165] epitaxically grown on Cu(1 0 0) (film thickness $\approx$10 nm), time-resolved measurements after Cs adsorption have also been performed [166]. Within the time resolution of the experimental set-up (5 fs), no difference in the decay dynamics of the alkali excitation compared to that of metal bulk excitation could be found. However, none of these films exhibits a (1 1 1) orientation, which is obviously the most favourable orientation for the stabilisation of the alkali resonance in case of the noble metal. No conclusive results exist for alkali adsorption on transition metals that allow statements on the alkali resonance lifetime as compared to the model studies for noble metals.

A specific aspect of the magnetic properties of Co, Ni, and Fe substrates should now be discussed. The respective band structures of these ferromagnetic systems split into two differently occupied spin sub-bands (majority band and minority band) which are a few eV apart [167]. Therefore, a decay of the alkali resonance depending on the spin state of the excited electron can be expected: RCT and electron–electron scattering for electrons with 'majority' spin should be different compared to 'minority' spin electrons, as the d-band overlap with the Fermi edge for the majority band is less pronounced (Fe) or even completely suppressed (Co, Ni). So far, neither the above mentioned real time experiments or the spin-dependent line width measurement of the cesium resonance indicate such kinds

of effect. The accuracy of the line width measurements is limited by the strong inhomogeneous broadening of the alkali resonances at elevated temperatures as mentioned above (the experiments were performed at 300 K). A higher sensitivity to these processes would be achieved in experiments at much lower temperatures.

An adsorption system rather different from the alkali on noble metal systems is the alkali adsorption on graphite. This system has gained some interest in recent years, [168] motivated by the specific electronic properties of the substrate: graphite exhibits a quasi-2D electronic structure, is a semi metal and has a very low density of states near the Fermi-level (about 10^{-4}–10^{-5} lower than typical metals). Experimental results on photodesorption of potassium from graphite(0 0 0 1) and their theoretical analysis indicate a rather small resonance line width of the 4s level of 150 meV corresponding to a lifetime of at least about 5 fs [169], compared to 19 fs predicted for K/Cu(1 1 1) (see Table 3). This stabilisation of the alkali resonance may be attributed to the layered structure of the graphite, which inhibits electron propagation/transfer perpendicular to the (0 0 0 1) surface and is likely to partly suppress RCT from the alkali. The fundamental origin of the long-lived alkali state may therefore be similar to that for the alkali/noble metal case. For a detailed description the specific electronic properties of graphite have to be taken into account. In particular, for the graphite system, anomalous features in the relaxation dynamics of hot substrate electrons have been observed, which are not present in metals and could be assigned to specific features of the graphite band structure [170,171].

5.2.3. A molecular resonance on Cu: CO/Cu(1 1 1) and (1 0 0)

The free CO molecule exhibits a well known resonance of $^2\Pi$ symmetry, that can be formed by the transient capture of an electron around 1.7 eV into the molecular $2\pi^*$ orbital. Although this shape resonance is rather short lived (around 0.7 fs), it is very efficient in inducing a resonant vibrational excitation process [172–174]. This $CO^-(^2\Pi)$ resonance has been much studied over the past years in the CO/metal system; in particular, it has been invoked as a reaction intermediate in a few systems [175,176]. Noble metal surfaces were therefore very attractive as a possibility for getting long-lived CO^- ions and thus very efficient reaction intermediates.

Time resolved photoemission experiments on $CO^-(2\pi^*)$/Cu(1 1 1) [175,177,178] yielded lifetimes shorter than 5 fs, this limit being set by the impossibility to actually measure the too fast time dependence of the decay. It seems that in this system, although the CO resonance lies within the Cu(1 1 1) projected band gap, no long-lived state appears. This absence has been confirmed by a theoretical study of the $CO^-(2\pi^*)$/Cu(1 1 1) and Cu(1 0 0) systems [95,179] using a joined ab initio/coupled angular mode (CAM) method (see e.g., Ref. [16,180] for a description of the CAM method applied to molecular resonances). A DFT study also confirmed the short lifetime of the CO resonance on Cu(1 1 1) and (1 0 0) resonance [181]. Fig. 14 presents the width of the $CO^-(2\pi^*)$ resonance on the Cu(1 1 1), (1 0 0) and on a free-electron metal surface, as a function of the molecule–surface distance. On both surfaces, at the adsorption distance (around 3.0 a_0), the level lifetime is seen to be extremely short, around 0.25 fs, even shorter than in the free molecule. It is very similar to that found on a free-electron metal, despite the presence of the projected band gap. This result allows for a more precise view of the conditions for the existence of a long-lived state induced by a projected band gap (see a detailed discussion in Ref. [95]). Two main features of the $CO^-(2\pi^*)$ state account for the difference with the alkali case: (i) the $CO^-(2\pi^*)$ resonance is a negative ion state and therefore the polarisation

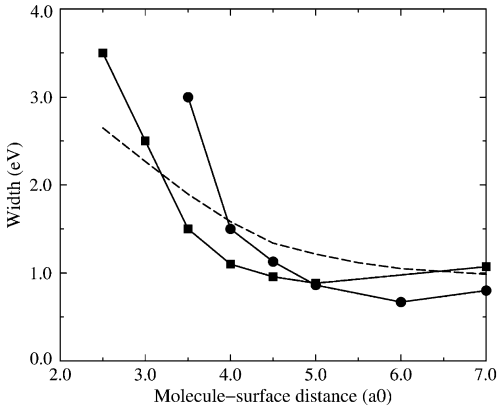

Fig. 14. Width of the $CO^{-}(2\pi^{*})$ resonance of the CO molecule adsorbed on a Cu surface, as a function of the molecule surface distance measured from the surface image plane. The molecular axis is normal to the surface. Dashed line: free-electron metal surface. Black squares: model Cu(1 1 1) surface. Black circles: model Cu(1 0 0) surface. (from Ref. [179]).

of the electronic cloud due to the interaction with the image charges will be the opposite of that observed in the case of a neutral alkali atom interacting with a metal; namely, the electronic cloud is attracted toward the surface. This distortion of the electronic cloud should strongly hamper the RCT blocking effect of the band gap. And (ii) the free $CO^{-}(2\pi^{*})$ state is quasi-stationary and therefore its decay is significantly different from that of an alkali atom that is stable for infinite atom–surface distances and only decays by tunnelling at finite distances. In the free molecule, the $CO^{-}(2\pi^{*})$ resonance can decay by emitting an electron in all directions of space, it is thus less influenced by what happens along the surface normal than an atom decaying via a tunnelling process, which is strongly favoured along the normal. Features (i) and (ii) make the RCT blocking effect much weaker in the $CO^{-}(2\pi^{*})$ case than in the case of an alkali and thus account for the short-lived state found in the $CO^{-}(2\pi^{*})$ case. We can then define the best situation for the existence of a long-lived state in an adsorbate/noble metal system: a neutral excited adsorbate, highly polarisable with a not too low level in the projected band gap.

5.3. Possible control scenarios of surface reactions

In the introductory section it was stated that an understanding of the mechanisms responsible for a long-lived excited state will enable one to control reactions at surfaces in the future. In the following two sections we will briefly discuss two potential approaches to experimentally realise such a control of surface chemistry.

5.3.1. Coherent control of alkali excitation and nucleus motion

Most attention so far in this review has been paid to the aspect of depopulation of the excited alkali resonance by means of RCT and e–e scattering processes. The second dynamical parameter, the total dephasing time T_2 has been considered much less, so far. One experimental study [12] reported an almost temperature independent dephasing time of the order of 10 fs for Cs/Cu(1 1 1), in agreement with the homogeneous line-width

of 70 meV which has been measured for this resonance at a temperature of 33 K. This value is of importance as it is long enough to allow a defined manipulation of the excitation process (coherent control) by the use of phase-controlled ultra-short excitation pulses. Consequently, it allows for a defined control of the nucleus motion/reaction process following the (laser-induced) electronic excitation of the alkali. In an early study, the possibility for this kind of manipulations was verified experimentally for Cs/Cu(1 1 1) [182]. It could be shown that depending on the relative phase of two temporally overlapping pulses the spectral 2PPE distribution from the Cs resonance can be significantly altered. Application of pulse-shaping techniques in combination with optimisation algorithms based on evolutionary strategies may in the future enable one to tailor reaction channels and efficiency in this kind of model type adsorption systems. In contrast to surface science, quantum control via pulse-shaping techniques have been used for the control of molecules in gas phase for some time now [183–185].

5.3.2. Interaction of alkali adsorbates with quantum well states – an alternative way to tune adsorbate–surface interaction

As we have seen in Section 4.1.4 it is not an easy task to experimentally separate the different contributions (RCT, e–e scattering, interaction with 2D surface bands, etc...) to the lifetime of the excited alkali state. This was important e.g., when the dependence on alkali coverage was discussed. The well-considered choice of the alkali/surface system can help to overcome this problem to a certain extent. Alkali adsorption on (1 1 1) oriented noble metal surfaces allows one to almost completely inhibit the RCT process, the dominant decay channel for other systems. Consequently, the relevance and strength of competing decay channels can be probed for these systems. As discussed above, other adsorption systems may be potential candidates for similar properties and are already being investigated. However, the next and more challenging step would be to gain direct access to a system intrinsic parameter that determines the strength of the adsorbate–substrate coupling. For example, one can think of tuning the strength of RCT by adjusting the substrate bulk states in resonance with the alkali excitation. One actual mean that could allow such an external tuning of electronic properties is the use of thin metal films. In this particular case, it has been shown that the electronic structure of a thin metallic film changes with the film thickness. For thin films, discrete quantum well states (QWS) appear in the electronic structure and have been observed for a number of different systems [186]. These quantum well states result from the quantisation of the electron motion perpendicular to the surface and represent a 2D continuum parallel to the surface. The energy of these states is determined by the film thickness and can be varied. With increasing coverage, these quantised states continuously transform into the bulk 3D continuum. QWS-tuning is a potential approach for an adjustment of the different decay channels of excited alkali states. Depending of the relative energy position of the QWS and of the adsorbate state, the number of QWS available for RCT decay varies, as well as the position of the resonance inside each continuum. The energy position of the resonance in each 2D continuum determines the $k_{\parallel}$ of the electron involved in the RCT decay, possibly leading to a partial blocking of the RCT in a way similar to that in the noble metal case. This aspect appears very clearly in theoretical investigations of this problem and shows that the RCT decay rate of an atom in front of a thin free-electron metallic film exhibits large variations following the excited state energy position just above or below a QWS [187–189]. The conditions for observing this finite size effect have been discussed, both for static and dynamic

situations [189]. The energy variation of the excited state can be obtained via a variation of the film thickness, possibly opening the way to a tuning of an adsorbate resonance. In this context, one can also mention that the inelastic electron–electron interaction is also different in a 2D or in a 3D system, as has been recently shown [190] and this can also influence the electron–electron interaction part of the decay of an adsorbate excited state. This brief discussion illustrates the two-fold interest of these reduced dimension systems: as a way to gain more detailed insight in the relaxation dynamics of excited adsorbates and as a potential means to build long-lived excited states.

Thin insulator layers on a metal surface, in particular rare gas layers, have also been found to deeply influence the lifetime of excited states at surfaces. If the excited state energy lies inside the insulator band gap, then penetration of the excited electron through the insulator layer has a low probability, weakening the decay of the excited state by RCT or inelastic electron scattering. The insulator layer then acts as a spacer layer, efficiently separating the excited state from the bulk substrate. This effect has been found in a few systems and has been proposed as a way to control excited state lifetimes. The effect of a spacer layer in increasing excited states lifetimes at surfaces has been used to explain a few different phenomena: vibrational excitation of molecules by resonant electron scattering in the case of molecules adsorbed on a thin insulator layer [191–193], energies and lifetimes of image states on metal surfaces covered by a thin rare gas layer [194–199], and survival against RCT of ions desorbing through an insulator layer in an electron stimulated desorption (ESD) experiment [200,201]. This effect has been modeled via the 1D-continuous dielectric medium (CDM) model [202,193,196,197,203,204] as well as via a 3D-microscopic approach [198].

6. Conclusions

We have presented a review on the properties of the long-lived alkali-induced excited states on noble metals. The model character of the alkali/metal systems allows one to obtain a good understanding of the various phenomena playing a role in the time evolution of these excited states and of the origin of their long lifetimes. Since the lifetime is the key parameter for excited state mediated surface reactions, it was of paramount importance to understand the origin of the long-lived excited states in certain adsorbate/metal systems. An interesting development would be a systematic study correlating lifetime measurements of the alkali-induced states and alkali desorption yield measurements, as an example of an excited state mediated surface reaction. To go beyond the present understanding of the excited state lifetime, studies of the dephasing time would be extremely helpful and could be linked with control attempts following the work of Petek et al. [182]. Finally, the analysis of the alkali/noble metal system yielded the conditions for a long-lived adsorbate-induced state: a polarisable neutral state located not too low inside the substrate surface-projected band gap. One may then wonder about the possibilities of finding new systems with long lifetimes and the possibility of tailoring them. In this end, adsorption on layered systems seems an attractive system to investigate. Adsorption on a thin insulator spacer layer on a metal substrate can be very efficient in decoupling the adsorbate and the metal states, thus leading to a strong increase of the excited state lifetimes. Adsorption on layered metal-on-metal systems is also very attractive since the lifetime of adsorbate-induced resonances could be influenced by their relative energy position with respect to quantum-well states in the layered system.

References

[1] R.R. Cavanagh, D.S. King, J.C. Stephenson, T.F. Heinz, J. Phys. Chem. 97 (1993) 786.
[2] J.W. Gadzuk, Surf. Sci. 342 (1995) 345.
[3] S. Deliwala, R.J. Finlay, J.R. Goldmann, T.H. Her, W.D. Miher, E. Mazur, Chem. Phys. Lett. 242 (1995) 617.
[4] L.M. Struck, L.J. Richter, S.A. Buntin, R.R. Cavanagh, J.C. Stephenson, Phys. Rev. Lett. 77 (1996) 4576.
[5] W. Ho, J. Phys. Chem. 100 (1996) 13050.
[6] M. Bonn, S. Funk, Ch. Hess, D.N. Denzler, C. Stampfl, M. Scheffler, M. Wolf, G. Ertl, Science 285 (1999) 1042.
[7] L. Sanche, J. Phys. B. 23 (1990) 1597.
[8] R.E. Palmer, Prog. Surf. Sci. 41 (1992) 51.
[9] J.W. Gadzuk, Chem. Phys. 251 (1999) 87.
[10] M. Bauer, S. Pawlik, M. Aeschlimann, Phys. Rev. B 55 (1997) 10040.
[11] M. Bauer, S. Pawlik, M. Aeschlimann, Phys. Rev. B 60 (1999) 5016.
[12] S. Ogawa, H. Nagano, H. Petek, Phys. Rev. Lett. 82 (1999) 1931.
[13] A.G. Borisov, A.K. Kazansky, J.P. Gauyacq, Surf. Sci. 430 (1999) 165.
[14] J.J.C. Geerlings, J. Los, Phys. Rep. 190 (1990) 133.
[15] P. Nordlander, J.C. Tully, Phys. Rev. Lett. 61 (1988) 990.
[16] D. Teillet-Billy, J.P. Gauyacq, Surf. Sci. 239 (1990) 343.
[17] V.A. Ermoshin, A.K. Kazansky, Phys. Lett. A 218 (1996) 99.
[18] S.A. Deutscher, X. Yang, J. Burgdörfer, Phys. Rev. A 55 (1997) 466.
[19] P. Kürpick, U. Thumm, U. Wille, Nucl. Inst. Methods B 125 (1997) 273.
[20] A.G. Borisov, D. Teillet-Billy, J.P. Gauyacq, Phys. Rev. Lett. 68 (1992) 2842.
[21] A.G. Borisov, D. Teillet-Billy, J.P. Gauyacq, H. Winter, G. Dierkes, Phys. Rev. B 54 (1996) 17166.
[22] S.B. Hill, CB. Haich, Z. Zhou, P. Nordlander, F.B. Dunning, Phys. Rev. Lett. 85 (2000) 5444.
[23] P.M. Echenique, J.M. Pitarke, E.V. Chulkov, A. Rubio, Chem. Phys. 251 (2000) 1.
[24] P.M. Echenique, J.B. Pendry, J. Phys. C 11 (1978) 2065.
[25] M.C. Desjonquères, D. Spanjaard, Surf. Sci. 40 (1993).
[26] H.D. Hagstrum, Phys. Rev. 96 (1954) 325.
[27] H.D. Hagstrum, Phys. Rev. 96 (1954) 336.
[28] N. Lorente, R. Monreal, Surf. Sci. 370 (1997) 324.
[29] M.A. Cazalilla, N. Lorente, R. Díez Muiño, J.P. Gauyacq, D. Teillet-Billy, P.M. Echenique, Phys. Rev. B 58 (1998) 13991.
[30] R.A. Baragolia, C.A. Dukes, Phys. Rev. Lett. 76 (1996) 2547.
[31] R. Monreal, Surf. Sci. 388 (1997) 231.
[32] Yu. Bandourine, S.S. Pop, S. Lacombe, L. Guillemot, V.A. Esaulov, Surf. Sci. 513 (2002) L413.
[33] R.W. Schoenlein, W.Z. Lin, J.G. Fujimoto, G.L. Eesley, Phys. Rev. Lett. 58 (1987) 1680.
[34] W.S. Fann, R. Storz, H.W.K. Tom, J. Bokor, Phys. Rev. B 46 (1992) 13592.
[35] B. Hellsing, J. Carlsson, L. Walldén, S.-Å. Lindgren, Phys. Rev. B 61 (2000) 2343.
[36] B. Hellsing, A. Eiguren, F. Reinert, G. Nicolay, E.V. Chulkov, V.M. Silkin, S. Hüfner, P.M. Echenique, J. Electron Spectrosc. Rel. Phen. 129 (2003) 97.
[37] A. Eiguren, B. Hellsing, F. R einert, G. Nicolay, E.V. Chulkov, V.M. Silkin, S. Hüfner, P.M. Echenique, Phys. Rev. Lett. 88 (2002) 066805.
[38] B. Hellsing, A. Eiguren, E.V. Chulkov, J. Phys. Condens. Matter 14 (2002) 5959.
[39] A. Hotzel, M. Wolf, J.P. Gauyacq, J. Phys. Chem. 104 (2000) 8438.
[40] A. Eiguren, B. Hellsing, E.V. Chulkov, P.M. Echenique, Phys. Rev. B 67 (2003) 235423.
[41] H.P. Bonzel, A.M. Bradshaw, G. Ertl (Eds.), Physics and Chemistry of Alkali Adsorption, Elsevier, New York, 1989.
[42] R.D. Diehl, R. Mc Grath, Surf. Sci. Rep. 23 (1996) 43.
[43] R.W. Gurney, Phys. Rev. 47 (1935) 479.
[44] N.D. Lang, A.R. Williams, Phys. Rev. 18 (1978) 616.
[45] H. Ishida, Phys. Rev. B 38 (1988) 8006.
[46] H. Ishida, T. Terakura, Phys. Rev. B 38 (1988) 5752.
[47] D.M. Riffe, G.K. Wertheim, P.H. Citrin, Phys. Rev. Lett. 64 (1990) 571.
[48] M. Scheffler, CH. Doste, A. Fleszar, F. Maca, G. Wachutka, G. Barzel, Physica B 172 (1991) 143.

[49] J. Bormet, J. Neugebauer, M. Scheffler, Phys. Rev. B 49 (1994) 17242.
[50] M. Scheffler, C. Stampfl, in: K. Horn, M. Scheffler (Eds.), Electronic structure, Handbook of Surface Science, Vol. 2, Elsevier Science, Amsterdam, 2000, p. 285.
[51] J. Neugebauer, M. Scheffler, Phys. Rev. Lett. 71 (1993) 577.
[52] J.N. Andersen, E. Lundgren, R. Nyholm, M. Qvarford, Surf. Sci. 289 (1993) 307.
[53] J.V. Barth, R.J. Behm, G. Ertl, Surf. Sci. 341 (1995) 62.
[54] J. Lehmann, P. Roos, E. Bertel, Phys. Rev. B 54 (1996) R2347.
[55] S.Å. Lindgren, L. Walldén, Phys. Rev. B 38 (1988) 3060.
[56] A. Carlsson, B. Hellsing, S.Å. Lindgren, L. Walldén, Phys. Rev. B 56 (1997) 1593.
[57] G. Hoffmann, R. Berndt, P. Johansson, Phys. Rev. Lett. 90 (2003) 046803.
[58] N. Memmel, G. Rangelov, E. Bertel, V. Dose, Phys. Rev. B 43 (1991) 6938.
[59] L.-A. Salmi, M. Persson, Phys. Rev. B RC 39 (1989) 6249.
[60] J.M. Carlsson, B. Hellsing, Phys. Rev. B 61 (2000) 13973.
[61] S.Å. Lindgren, L. Walldén, Solid State Commun. 25 (1978) 13.
[62] P. Soukiassian, R. Riwan, J. Lecante, E. Wimmer, S.R. Chubb, A.J. Freeman, Phys. Rev. B 31 (1985) 4911.
[63] W. Jacob, E. Bertel, V. Dose, Phys. Rev. B 35 (1987) 5910.
[64] D. Heskett, K.-H. Frank, K. Horn, E.E. Koch, H.-J. Freund, V. Baddorf, K.-D. Tsuei, E.W. Plummer, PRB 37 (1988) 10387.
[65] S. Reiff, W. Drachsel, J.H. Block, Surf. Sci. Lett. 304 (1994) L420.
[66] N. Fischer, S. Schuppler, Th. Fauster, W. Steinmann, Surf. Sci. 314 (1994) 89.
[67] Th. Fauster, W. Steinmann, in: P. Halevi (Ed.), Photonic Probes of Surfaces, Electromagnetic Waves: Recent Developments in Research, Vol. 2, North-Holland, Amsterdam, 1995, p. 347.
[68] S.D. Kevan, Phys. Rev. Lett. 50 (1983) 526.
[69] J.A.D. Matthew, F.P. Netzer, G. Astl, Surf. Sci. Lett. 259 (1991) L757.
[70] R. Dudde, L.S.O. Johansson, B. Reihl, Phys. Rev. B 44 (1991) 1198.
[71] S.Å. Lindgren, L. Walldén, Solid State Commun. 34 (1980) 671.
[72] D. Tang, D. Heskett, Phys. Rev. B 47 (1993) 10695.
[73] D. Tang, C. Su, D. Heskett, Surf. Sci. 295 (1993) 427.
[74] D.A. Arena, F.G. Curti, R.A. Bartinsky, Phys. Rev. B 56 (1997) 15404.
[75] H.B. Nielsen, W. Thowladda, Surf. Sci. Lett. 284 (1993) L426.
[76] K.-H. Frank, H.-J. Sagner, D. Heskett, Phys. Rev. B 40 (1989) 2767.
[77] M. Bauer, Ph.D. thesis, University of Zurich, 1997.
[78] M. Bauer, S. Pawlik, R. Burgermeister, M. Aeschlimann, Surf. Sci. 402–404 (1998) 62.
[79] H. Petek, H. Nagano, M.J. Weida, S. Ogawa, J. Phys. Chem. B 105 (2001) 6767.
[80] G.K. Wertheim, D.M. Riffe, P.H. Citrin, Phys. Rev. B 49 (1994) 4834.
[81] N.D. Lang, in: H.P. Bonzel, A.M. Bradshaw, G. Ertl (Eds.), Physics and Chemistry of Alkali Metal Adsorption, Elsevier, New York, 1989.
[82] J.P. Muscat, D.M. Newns, Surf. Sci. 84 (1979) 262.
[83] J.P. Muscat, D.M. Newns, Surf. Sci. 74 (1978) 355.
[84] P. Nordlander, J.C. Tully, Phys. Rev. B 42 (1990) 5564.
[85] J. Sjakste, A.G. Borisov, J.P. Gauyacq, Nucl. Inst. Methods B 203 (2003) 49.
[86] E. Lundgren, A. Beutler, R. Nyholm, J.N. Andersen, D. Heskett, Surf. Sci. 370 (1997) 311.
[87] C. Stampfl, J. Neugebauer, M. Scheffler, Surf. Sci. 307 (1994) 8.
[88] H. Petek, S. Ogawa, Progress Surf. Sci. 56 (1997) 239.
[89] T. Hertel, E. Knoesel, M. Wolf, G. Ertl, Phys. Rev. Lett. 76 (1996) 535.
[90] M.J. Weida, S. Ogawa, H. Nagano, H. Petek, J. Opt. Soc. Am. B 17 (2000) 1443.
[91] T. Hecht, H. Winter, A.G. Borisov, J.P. Gauyacq, A.K. Kazansky, Phys. Rev. Lett. 84 (2000) 2517.
[92] A.G. Borisov, A.K. Kazansky, J.P. Gauyacq, Phys. Rev. B 59 (1999) 10935.
[93] L. Kleinman, D.M. Bylander, Phys. Rev. Lett. 48 (1982) 1425.
[94] J.N. Bardsley, Case studies in Atomic Phys. 4 (1974) 299.
[95] J.P. Gauyacq, A.G. Borisov, G. Raşeev, A.K. Kazansky, Faraday Discussions 117 (2000) 15.
[96] P.J. Jennings, P.O. Jones, M. Weinert, Phys. Rev. B. 37 (1988) 6113.
[97] E.V. Chulkov, V.M. Silkin, P.M. Echenique, Surf. Sci. 437 (1999) 330.
[98] E.V. Chulkov, V.M. Silkin, P.M. Echenique, Surf. Sci. 391 (1997) L1217.
[99] M.D. Fleit, J.A. Fleck, J. Chem. Phys. 78 (1982) 301.
[100] R. Kosloff, J. Phys. Chem. 92 (1988) 2087.

[101] A.G. Borisov, J.P. Gauyacq, A.K. Kazansky, E.V. Chulkov, V.M. Silkin, P.M. Echenique, Phys. Rev. Lett. 86 (2001) 488.
[102] A.G. Borisov, J.P. Gauyacq, A.K. Kazansky, E.V. Chulkov, V.M. Silkin, P.M. Echenique, Phys. Rev. B 65 (2002) 235434.
[103] L. Hedin, S. Lundqvist, Solid State Phys. 23 (1969) 1.
[104] E.V. Chulkov, V.M. Silkin, M. Machado, Surf. Sci. 482–485 (2001) 693.
[105] M.A. Van Hove, W.H. Weinberg, C.M. Chan, in: Low Energy Electron Diffraction, Springer, Berlin, 1986.
[106] M. Aeschlimann, M. Bauer, S. Pawlik, Chem. Phys. 205 (1996) 127.
[107] S.Å. Lindgren, L. Wallden, Phys. Rev. B 28 (1983) 6707.
[108] W. Mannstadt, G. Grawert, Phys. Rev. B 52 (1995) 5343.
[109] CRC Handbook of Chemistry and Physics, CRC Press, Boca Raton, 1996.
[110] A.G. Borisov, G. Makhmetov, D. Teillet-Billy, J.P. Gauyacq, Surf. Sci. 350 (1996) L205.
[111] D. Goryunov, A.G. Borisov, G. Makhmetov, D. Teillet-Billy, J.P. Gauyacq, Surf. Sci. 401 (1998) 206.
[112] J.P. Gauyacq, A.G. Borisov, J. Phys. C 10 (1998) 6585.
[113] P.J. Rous, Phys. Rev. Lett. 74 (1995) 1835.
[114] A. Hotzel, K. Ishioka, E. Knoesel, M. Wolf, G. Ertl, Chem. Phys. Lett. 285 (1998) 271.
[115] S. Gao, D.C. Langreth, Surf. Sci. 398 (1998) L314.
[116] P. Hyldgaard, M. Persson, J. Phys.: Condens. Matter 12 (2000) L13.
[117] J. Osma, I. Sarria, E.V. Chulkov, J.M. Pitarke, P.M. Echenique, Phys. Rev. B 59 (1999) 10591.
[118] A.G. Borisov, D. Teillet-Billy, J.P. Gauyacq, Nucl. Inst. Methods B 78 (1993) 49.
[119] S.Å. Lindgren, L. Walldén, Surf. Sci. 89 (1979) 319.
[120] D. Menzel, R. Gomer, J. Chem. Phys. 41 (1964) 3311.
[121] P.A. Redhead, Can. J. Phys. 42 (1964) 886.
[122] H. Petek, M.J. Weida, H. Nagano, S. Ogawa, Science 288 (2000) 1402.
[123] B. Hellsing, D.V. Chakarov, L. Österlund, V.P. Zhdanov, B. Kasemo, J. Phys.Chem. 106 (1997) 982.
[124] A.G. Borisov, A.K. Kazansky, J.P. Gauyacq, Phys. Rev. B Rapid Commun. 64 (2001) 201105.
[125] K. Jacobi, H. Shi, M. Gruyters, G. Ertl, Phys. Rev. B 49 (1994) 5733.
[126] P. Senat, J.P. Toennies, G. Witte, Chem. Phys. Lett. 299 (1999) 389.
[127] A.K. Kazansky, A.G. Borisov, J.P. Gauyacq, Surf. Sci. 577 (2005) 47.
[128] J.P. Gauyacq, A.K. Kazansky, Phys. Rev. B 72 (2005) 045418.
[129] M. Bauer, M. Wessendorf, D. Hoffmann, C. Wiemann, A. Mönnich, M. Aeschlimann, Appl. Phys. A 80 (2005) 987.
[130] A.G. Borisov, A.K. Kazansky, J.P. Gauyacq, Phys. Rev. Lett. 80 (1998) 1996.
[131] L. Guillemot, V. Esaulov, Phys. Rev. Lett. 82 (1999) 4552.
[132] A.R. Canario, A.G. Borisov, J.P. Gauyacq, V.A. Esaulov, Phys. Rev. B 71 (2005) 121401(R).
[133] J.N.M. Van Wunnick, R. Brako, K. Makoshi, D.M. Newns, Surf. Sci. 126 (1983) 618.
[134] H. Winter, Commun. Atom. Mol. Phys. 26 (1991) 287.
[135] T. Hecht, H. Winter, A.G. Borisov, J.P. Gauyacq, A.K. Kazansky, Faraday Discussion 117 (2000) 27.
[136] A.G. Borisov, A.K. Kazansky, J.P. Gauyacq, Phys. Rev. B 65 (2002) 205414.
[137] A.G. Borisov, A.K. Kazansky, J.P. Gauyacq, unpublished.
[138] A.G. Borisov, A.K. Kazansky, J.P. Gauyacq, Surf. Sci. 505 (2002) 260.
[139] A.G. Borisov, A.K. Kazansky, J.P. Gauyacq, Surf. Sci. 526 (2003) 72.
[140] B. Simon, Annal. Phys. 97 (1976) 279.
[141] H. Namba, N. Nakanishi, T. Yamagushi, H. Juroda, Phys. Rev. Lett. 71 (1993) 4027.
[142] J.E. Ortega, F.J. Himpsel, R. Haight, D.R. Peale, Phys. Rev. B 49 (1994) 13859.
[143] X.J. Shen, H. Kwak, D. Mocuta, A.M. Radojevic, S. Smadici, R.M. Osgood Jr., Phys. Rev. B 63 (2001) 165403.
[144] L. Bartels, S.W. Hla, A. Kühnle, G. Meyer, K.-H. Rieder, Phys. Rev. B 67 (2003) 205416.
[145] J.P. Gauyacq, A.G. Borisov, A.K. Kazansky, Appl. Phys. A 78 (2004) 141.
[146] F.E. Olsson, M. Persson, A.G. Borisov, J.P. Gauyacq, J. Lagoute, S. Fölsch, Phys. Rev. Lett. 93 (2004) 206803.
[147] V. Madhavan, W. Chen, T. Jamneala, M.F. Crommie, N.S. Wingreen, Science 280 (1998) 567.
[148] V. Madhavan, W. Chen, T. Jamneala, M.F. Crommie, Phys. Rev. B 64 (2001) 165412.
[149] L. Limot, E. Pehlke, J. Kröger, R. Berndt, Phys. Rev. Lett. 94 (2005) 036805.
[150] V.S. Stepanyuk, A.N. Klavsyuk, L. Niebergall, P. Bruno, Phys. Rev. B 72 (2005) 153407.
[151] J. Tersoff, S.D. Kevan, Phys. Rev. B 28 (1983) 4267.

[152] X.Y. Wang, R. Paiella, R.M. Osgood Jr., Phys. Rev. B 51 (1995) 17035.
[153] C. Reuss, I.L. Shumay, U. Thomann, M. Kutschera, M. Weinelt, Th. Fauster, U. Höfer, Phys. Rev. Lett. 82 (1999) 153.
[154] Th. Fauster, C. Reuss, I.L. Shumay, M. Weinelt, Chem. Phys. 251 (2000) 111.
[155] M. Weinelt, Surf. Sci. 482–485 (2001) 519.
[156] G.C. King, M. Tronc, F.H. Read, R.C. Bradford, J. Phys. B 10 (1977) 2479.
[157] C. Keller, M. Stichler, G. Comelli, F. Esch, S. Lizzit, W. Wurth, D. Menzel, Phys. Rev. Lett. 80 (1998) 1774.
[158] A. Kivimäki, A. Naves de Brito, S. Aksela, H. Aksela, O.-P. Sairanen, A. Ausmees, S.J. Osborne, L.B. Dantas, S. Svensson, Phys. Rev. Lett. 71 (1993) 4307.
[159] S. Sundin, F.Kh. Gel'mukhanov, H. Ågren, S.J. Osborne, A. Kikas, O. Björneholm, A. Ausmees, S. Svensson, Phys. Rev. Lett. 79 (1997) 1451.
[160] O. Karis, A. Nilsson, M. Weinelt, T. Wiell, C. Puglia, N. Wassdahl, N. Mårtensson, M. Samant, J. Stöhr, Phys. Rev. Lett. 76 (1996) 1380.
[161] A. Sandell, P.A. Brühwiler, A. Nilsson, P. Bennich, P. Rudolf, N. Mårtensson, Surf. Sci. 429 (1999) 309.
[162] W. Wurth, D. Menzel, Chem. Phys. 251 (2000) 141.
[163] A. Föhlisch, D. Menzel, P. Feulner, M. Ecker, R. Weimar, K.L. Kostov, G. Tyuliev, S. Lizzit, R. Larciprete, F. Hennies, W. Wurth, Chem. Phys. 289 (2003).
[164] J.P. Gauyacq, A.G. Borisov, Phys. Rev. B 69 (2004) 235408.
[165] M. Aeschlimann, M. Bauer, S. Pawlik, W. Weber, R. Burgermeister, D. Oberli, H.C. Siegmann, Phys. Rev. Lett. 79 (1997) 5158.
[166] M. Bauer, S. Pawlik, R. Burgermeister, M. Aeschlimann, unpublished.
[167] J. Callaway, C.S. Wang, Phys. Rev. B 7 (1973) 1096.
[168] L. Österlund, D.V. Chakarov, B. Kasemo, Surf. Sci. 420 (1999) 174, and references in there.
[169] B. Hellsing, D.V. Chakarov, L. Österlund, V.P. Zhdanov, B. Kasemo, J. Chem. Phys. 106 (1997) 982.
[170] G. Moos, C. Gahl, R. Fasel, M. Wolf, T. Hertel, Phys. Rev. Lett 87 (2001) 267402.
[171] C.D. Spataru, M.-A. Cazalilla, A. Rubio, L. Benedict, P.M. Echenique, S.G. Louie, Phys. Rev. Lett. 87 (2001) 246405.
[172] G.J. Schulz, Rev. Mod. Phys. 45 (1973) 423.
[173] H. Ehrhardt, L. Langhaus, F. Linder, H.S. Taylor, Phys. Rev. 173 (1968) 222.
[174] M. Tronc, R. Azria, Y. Le Coat, J. Phys. B 13 (1980) 2327.
[175] L. Bartels, G. Meyer, K.-H. Rieder, D. Velic, E. Knoesel, A. Hotzel, M. Wolf, G. Ertl, Phys. Rev. Lett. 80 (1998) 2004.
[176] D. Bejan, G. Raşeev, M. Monnerville, Surf. Sci. 470 (2001) 293.
[177] T. Hertel, E. Knoesel, E. Hasselbrink, M. Wolf, G. Ertl, Surf. Sci. 317 (1994) L1147.
[178] E. Knoesel, T. Hertel, M. Wolf, G. Ertl, Chem. Phys. Lett. 240 (1995) 409.
[179] J.P. Gauyacq, A.G. Borisov, G. Raşeev, Surf. Sci. 490 (2001) 99.
[180] V. Djamo, D. Teillet-Billy, J.P. Gauyacq, Phys. Rev. Lett. 71 (1993) 3267;
V. Djamo, D. Teillet-Billy, J.P. Gauyacq, Phys. Rev. B 51 (1995) 5418.
[181] N. Lorente, M. Persson, Excited States Surf. 117 (2000) 277.
[182] H. Petek, H. Nagano, M.J. Weida, S. Ogawa, J. Phys. Chem. A 104 (2000) 10234.
[183] L. Zhu, V. Kleimann, X. Li, S. Lu, K. Trentelmann, R.J. Gordon, Science 270 (1995) 77.
[184] A. Assion, T. Baumert, M. Bergt, T. Brixner, B. Kiefer, V. Seyfried, M. Strehle, G. Gerber, Science 282 (1998) 919.
[185] F. Legare, S. Chelkowski, A.D. Bandrauk, J. Raman Spectrosc. 31 (2000) 15.
[186] for an overview on quantum well states in thin metal films see T.-C. Chiang, Surf. Sci. Rep. 39 (2000) 181.
[187] A.G. Borisov, H. Winter, Z. Phys. D: Atom. Mol. Clusters 37 (1996) 253.
[188] B. Bahrim, P. Kürpick, U. Thumm, U. Wille, Nucl. Inst. Methods B 164–165 (2000) 614.
[189] E.Yu. Usman, I.F. Urazgil'din, A.G. Borisov, J.P. Gauyacq, Phys. Rev. B 64 (2001) 205405.
[190] L. Vitali, P. Wahl, M.A. Schneider, K. Kern, V.M. Silkin, E.V. Chulkov, P.M. Echenique, Surf. Sci. 523 (2003) L47.
[191] M. Michaud, L. Sanche, C. Gaubert, R. Baudoing, Surf. Sci. 205 (1988) 447.
[192] L. Sanche, A.D. Bass, P. Ayotte, I.I. Fabrikant, Phys. Rev. Lett. 75 (1995) 3568.
[193] D.C. Marinica, D. Teilllet-Billy, J.P. Gauyacq, M. Michaud, L. Sanche, Phys. Rev. B 64 (2001) 085408.
[194] D.F. Padowitz, W.R. Merry, C.E. Jordan, C.B. Harris, Phys. Rev. Lett. 69 (1992) 3583.
[195] M. Wolf, E. Knoesel, T. Hertel, Phys. Rev. B 54 (1996) R5295.
[196] A. Hotzel, G. Moos, K. Ishioka, M. Wolf, G. Ertl, Appl. Phys. B 68 (1999) 615.

[197] W. Berthold, U. Höfer, P. Feulner, D. Menzel, Chem. Phys. 251 (2000) 123.
[198] D.C. Marinica, C. Ramseyer, A.G. Borisov, D. Teillet-Billy, J.P. Gauyacq, W. Berthold, P. Feulner, U. Höfer, Phys. Rev. Lett. 89 (2002) 046802.
[199] C.D. Lindstrom, D. Quinn, X.-Y. Zhu, J. Chem. Phys. 122 (2005) 124714.
[200] N.J. Sack, M. Akbulut, T. Madey, Phys. Rev. B 51 (1995) 4585.
[201] N.J. Sack, M. Akbulut, T. Madey, Surf. Sci. 334 (1995) L695.
[202] M.W. Cole, Phys. Rev. B 3 (1971) 4418.
[203] J.D. Mc Neill, R.L. Lingle, R.E. Jordan, D.F. Padowitz, C.B. Harris, J. Chem. Phys. 105 (1996) 3883.
[204] P. Nordlander, J.P. Modisette, Nucl. Inst. Methods B 125 (1997) 305.
[205] M. Wiesenmayer, Diploma thesis, 2006.